AFRL-AFOSR-UK-TR-2012-0003

Short Range 10 Gb/s THz Communications Proof of Concept Phase 2

Alwyn J. Seeds

University College London
Department of Electronic and Electrical Engineering
Torrington Place
London, United Kingdom WC1E 7JE

EOARD GRANT 09-3078

Report Date: December 2011

Final Report from 17 August 2009 to 17 August 2011

Air Force Research Laboratory
Air Force Office of Scientific Research
European Office of Aerospace Research and Development
Unit 4515 Box 14, APO AE 09421

REPORT DOCUMENTATION PAGE

Form Approved OMB No. 0704-0188

1. REPORT DATE *(DD-MM-YYYY)*	2. REPORT TYPE	3. DATES COVERED *(From – To)*
09-12-2011	Final Report	17 August 2009 – 17 August 2011

4. TITLE AND SUBTITLE

Short Range 10 Gb/s THz Communications Proof of Concept Phase 2

5a. CONTRACT NUMBER

FA8655-09-1-3078

5b. GRANT NUMBER

Grant 09-3078

5c. PROGRAM ELEMENT NUMBER

61102F

6. AUTHOR(S)

Professor Alwyn J. Seeds

5d. PROJECT NUMBER

5d. TASK NUMBER

5e. WORK UNIT NUMBER

7. PERFORMING ORGANIZATION NAME(S) AND ADDRESS(ES)

University College London
Department of Electronic and Electrical Engineering
Torrington Place
London, United Kingdom WC1E 7JE

8. PERFORMING ORGANIZATION REPORT NUMBER

N/A

9. SPONSORING/MONITORING AGENCY NAME(S) AND ADDRESS(ES)

EOARD
Unit 4515 BOX 14
APO AE 09421

10. SPONSOR/MONITOR'S ACRONYM(S)

AFRL/AFOSR/RSW (EOARD)

11. SPONSOR/MONITOR'S REPORT NUMBER(S)

AFRL-AFOSR-UK-TR-2012-0003

12. DISTRIBUTION/AVAILABILITY STATEMENT

Approved for public release; distribution is unlimited.

13. SUPPLEMENTARY NOTES

14. ABSTRACT

This report results from a contract tasking University College London as follows: SHORT RANGE 10 GB/S THZ COMMUNICATIONS PROOF OF CONCEPT PHASE 2 PROPOSAL
This project has investigated the potential of photonic techniques for generating and coherently detecting millimetre and THz waves, with short-range (in-room) Gb/s communications systems that operate in unlicensed spectrum above 300 GHz as the target application. This would allow compact, low-cost transceivers to be fabricated that leverage the mature InP-based photonic component and integration technologies that have been developed for optical fibre communications. In this project, the UTC-PD has, for the first time, been investigated as a down-converting optoelectronic mixer, simplifying the receiver by combining the functions of LO generation and mixing in a single device with potential for monolithic integration with OHG components. Data transmission experiments were carried out in which a UTC-PD as a down-converting mixer or a data transmitter. BPSK was transmitted on an 80 GHz carrier at a rate of 500 kb/s. Also, optical heterodyne combining the outputs of two external cavity lasers and OOK-modulated at 1 Gb/s using an external electro-optic modulator was converted to a modulated signal at 200 GHz with a UTC-PD. The signal was transmitted over a short wireless link to a Schottky barrier diode mixer, to an IF of 2.5 GHz. Offline processing converted the signal to baseband and achieve a bit error rate (BER) of 10-3 at -52 dBm. Transmission with the same BER should be possible over link lengths of more than 1 m at 300 GHz. The results achieved in the project show the UTC-PDs, as sources and/or optoelectronic mixers, will be key in future high-data-rate wireless communication systems at low-THz carrier frequencies.

15. SUBJECT TERMS

EOARD, Laser amplifiers, Fibre Optics, Nonlinear Optics

16. SECURITY CLASSIFICATION OF:			17. LIMITATION OF ABSTRACT	18, NUMBER OF PAGES	19a. NAME OF RESPONSIBLE PERSON
a. REPORT	b. ABSTRACT	c. THIS PAGE			A. GAVRIELIDES
UNCLAS	UNCLAS	UNCLAS	SAR	36	19b. TELEPHONE NUMBER *(Include area code)* +44 (0)1895 616205

UCL DEPARTMENT OF ELECTRONIC &
ELECTRICAL ENGINEERING

SHORT RANGE 10 GB/S THZ COMMUNICATIONS PROOF OF CONCEPT

Award number
FA8655-09-1-3078

Final Report
October 2011

Martyn Fice
Efthymios Rouvalis
Robert Steed
Lalitha Ponnampalam
Chin-Pang Liu
Cyril Renaud
Alwyn Seeds

ABSTRACT

This project has investigated the potential of photonic techniques for generating and coherently detecting millimetre and THz waves, with short-range (in-room) Gb/s communications systems that operate in unlicensed spectrum above 300 GHz as the target application. The focus has been on the uni-travelling carrier (UTC) photodiode (PD), which has been investigated both as a source of modulated millimetre and THz wave signals, and, for the first time, as a down-converting optoelectronic mixer. Utilising the UTC-PD as a mixer could simplify integration with the other components required for photonic local oscillator generation, enabling compact THz receivers to be realised.

Key results from the project are summarised below:

- The UTC-PD has been demonstrated as a W-band (75 – 110 GHz) down-converting optoelectronic mixer for the first time.

- UTC-PD mixer characteristics for fundamental down-conversion from 100 GHz have been measured as:
  - Conversion gain as high as -32 dB (at 10 mA photocurrent and 4 V reverse bias).
  - Linear relationship between W-band and IF powers over more than 5 decades of power variation.
  - < 3 dB variation of IF power across the IF frequency range 5 – 10 GHz.

- Sub-harmonic mixing has been demonstrated using the UTC-PD in the following modes:
  - W-band RF / sub-harmonic optical.
  - W-band optical / sub-harmonic RF.

- Wide UTC-PD mixer IF bandwidth has been demonstrated by sub-harmonic mixing experiments: < 6 dB variation for IF from 5 – 23 GHz.

- Qualitative and quantitative models of optoelectronic mixing in UTC-PD have been developed.

- Data transmission experiments have been carried out using the UTC-PD as an optoelectronic down converter:
  - 500 kb/s BPSK on 80 GHz carrier over 5 cm.

- Data transmission experiments have been carried out using the UTC-PD as a transmitter:
  - 1 Gb/s OOK on 200 GHz carrier over ~2 cm using Schottky barrier diode down converter; bit error rate of 10^{-3} achieved for an estimated received power of -52 dBm.

COMPLIANCE WITH GRANT TERMS

Acknowledgement of Sponsorship

The Grantee accepts responsibility for assuring that an acknowledgement of Government support will appear in any publication of any material based on or developed under this project, in the following terms:

"Effort sponsored by the Air Force Office of Scientific Research, Air Force Material Command, USAF, under grant number FA8655-09-1-3078. The U.S. Government is authorized to reproduce and distribute reprints for Government purpose notwithstanding any copyright notation thereon."

Disclaimer

The Grantee accepts responsibility for assuring that every publication of material based on or developed under this project contains the following disclaimer:

"The views and conclusions contained herein are those of the author and should not be interpreted as necessarily representing the official policies or endorsements, either expressed or implied, of the Air Force Office of Scientific Research or the U.S. Government."

TABLE OF CONTENTS

LIST OF FIGURES

LIST OF TABLES

1 SUMMARY

The objective of this project was to investigate and demonstrate the potential of photonic techniques for generating and coherently detecting millimetre and THz waves, with short-range (in-room) Gb/s communications systems that operate in unlicensed spectrum above 300 GHz as the target application. In particular, the uni-travelling carrier (UTC) photodiode (PD) has been investigated experimentally as both a source of modulated millimetre or THz waves and, for the first time, as a down-converting optoelectronic mixer. Data transmission experiments have been performed using UTC-PDs in both roles.

In Phase 1 of the project (Award Number FA8655-07-1-3043), preliminary studies of using an UTC photodiode as an optoelectronic mixer were carried out at < 40 GHz (rather than THz) frequencies. That work was reported in the Final Report for that Award, dated November 2008, and is not repeated here.

Under this Award, in Phase 2 of the project, experimental and theoretical investigations were carried out into using the UTC as an optoelectronic mixer for down-converting data modulated signals on carriers in the THz range (>100 GHz). This work was continued in the final phase of the project (Phase 3), with high-speed (1 Gb/s) wireless transmission also being demonstrated over short range at THz carrier frequency (200 GHz).

For ease of reference, this report consolidates into a single document material from Phases 2 and 3 of the project. Work carried out since the Phase 3 Interim Report is reported in Sections 4.3.2 and 5.3.2 of this report, while the analysis of previously reported results is updated in Section 5.1.4.

2 INTRODUCTION

The THz frequency region potentially has a number of advantages for secure wireless communication. The stronger water absorption in this frequency range, compared to the standard wireless bands, limits transmission distance and allows the signal to be more easily confined, for instance within a building. Furthermore it offers a wide range of possible carrier frequencies; from 100 GHz to 1.5 THz for the system proposed.

For a THz communications system we require (1) a THz source that can conveniently be modulated at high speed (Gb/s), and (2) a high sensitivity THz detector from which the information can be demodulated.

Photonic generation of THz signals using telecommunications-based technologies provides a route to cheap, compact, highly efficient, room-temperature, Continuous Wave (CW) sources [1]. Heterodyning of two CW optical signals, each phase locked to lines in an optical comb, is used to generate modulation at THz frequencies, with the optical signal converted to THz radiation using a very wide bandwidth photodiode (PD) driving an antenna. The THz output can readily be modulated by modulating one of the CW optical signals before heterodyning, or by modulating the heterodyne optical signal. All of the major components could be integrated using InP technology to realise a compact, low-power-consumption THz transmitter.

Techniques generally used for THz detection and power measurement, for instance Golay cells, do not have fast enough response for high-speed data demodulation. Instead, it is necessary to down-convert the received THz signal to a much lower intermediate frequency (IF) where conventional electronics can be employed. This requires a suitable mixer to be employed, with the modulated THz signal received via a suitable antenna as one input (the “RF” input) and a THz local oscillator (LO) signal at a frequency offset by the IF. The use of this coherent detection approach also enables a large increase in sensitivity, which could enable THz frequency communication over reasonable distances, as it will help in overcoming water absorption in the air.

The mixer for frequency down-conversion requires a component that exhibits nonlinear characteristics. The UTC, because of its nonlinear current-voltage (IV) characteristic, is a candidate for such a mixer, in addition to being a high-speed photodiode. The modulated THz signal received by an antenna is fed to the diode electrical contacts, and a THz-modulated optical local oscillator, generated by an heterodyne method similar to that used in the transmitter source, is applied to the optical input, to form a convenient optoelectronic mixer in a single device.

The overall scheme proposed for the proof-of-concept THz communications system is thus as shown in Figure 1. On the left is the transmitter, based on heterodyne photonic THz generation. The two slave lasers to be heterodyned are phase locked to spectral lines selected from the optical frequency comb generator (OFCG) using optical phase locked loops (OPLLs) or by optical injection locking (OIL). Data modulation of the heterodyne signal can be applied either by modulating the output of one of the slave lasers before heterodyning or, as shown, by directly modulating the heterodyne signal itself. The modulated optical heterodyne signal is converted to a modulated THz-frequency signal by detection in a wide-bandwidth photodetector, such as a Travelling-Wave Uni-Travelling Carrier (TW-UTC) photodiode.

The OFCG, phase locked slave lasers, and high-bandwidth UTC photodiode for THz generation have all been demonstrated previously, and integration of these components is being investigated in other projects. The main novel element on the transmitter side to be demonstrated is the modulation of the THz signal by optical modulation.

The modulated THz data signal propagates over a short wireless link between two antennas to the receiver, shown on the right of Figure 1. The received THz signal is mixed with a THz LO in a second wide-bandwidth photodiode, to generate an IF carrying the data signal, which is then detected by standard RF techniques. The THz LO is shown schematically as being generated by a second optical heterodyne scheme similar to that used in the transmitter, although for experimental convenience this could be derived from the transmitter heterodyne using a suitable offset generation technique. The UTC photodiode acts as an optoelectronic mixer, combining the functions of generating the THz LO and mixing the THz signal and THz LO. Demonstrating that the UTC can be operated as an optoelectronic mixer and characterising its performance in this mode are key objectives for this project.

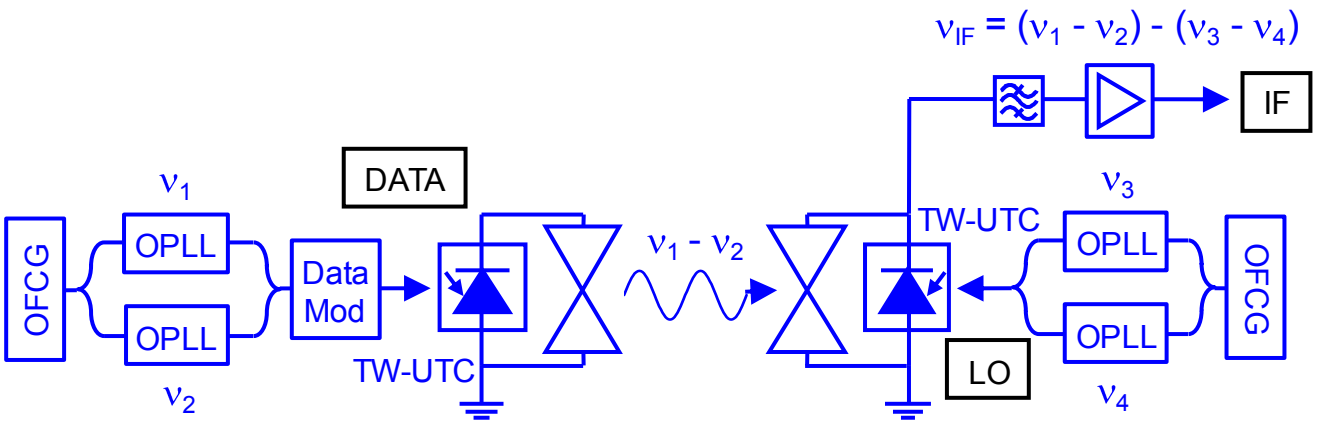

Figure 1: THz communications system.

3 PROJECT OBJECTIVES

As outlined in the previous section, the key objectives for the project are to:

1. Demonstrate the UTC as an optoelectronic mixer, and characterise its performance up to THz frequencies. Although the UTC has demonstrated excellent performance to 1 THz as a photodiode, it had not been investigated as an optoelectronic mixer prior to this project. Areas to be investigated include its frequency response in mixer mode, and practical issues related to extracting the modulated IF.
2. Demonstrate a data modulated THz source, with a target bit rate of 10 Gb/s.
3. Demonstrate coherent detection of the data modulated THz source using the UTC as an optoelectronic mixer.

In Phase 1 of the project (Award Number FA8655-07-1-3043), preliminary studies into using a UTC photodiode as an optoelectronic mixer were carried out at < 40 GHz (rather than THz) frequencies. This work was reported in the Final Report for that Award, dated November 2008, and is not repeated here.

Phase 2 of the project extended that work, with experimental and theoretical investigations of the UTC as an optoelectronic mixer for down-converting data modulated signals on carriers in the THz range (>100 GHz).

In the final phase (Phase 3), we continued investigation of the UTC photodiode as an optoelectronic mixer and demonstrated high-speed (1 Gb/s) wireless transmission over short range at low THz carrier frequency (200 GHz).

This report consolidates into a single document material from Phases 2 and 3 of the project. New results obtained since the Phase 3 Interim Report are reported in Sections 4.3.2 and 5.3.2 of this report, while the analysis of previously reported results is updated in Section 5.1.4.

4 METHODS, ASSUMPTIONS, AND PROCEDURES

4.1 Optoelectronic mixing in UTC photodiodes

A major activity in the project has been the experimental evaluation of UTC PDs as optoelectronic mixers in the W-band (75 GHz to 110 GHz). Since equipment is available commercially for this band, signal generation and analysis is simplified.

The experimental arrangement used for measuring the conversion gain of the UTC optoelectronic mixer is shown in Figure 2. The W-band signal to be down-converted was generated using a commercial x6 frequency multiplier and applied to the UTC using a W-band coplanar probe with waveguide input. To avoid mechanically stressing the coplanar probe, the multiplier output was coupled to the probe via two closely spaced 20 dBi horn antennas. The output power of the multiplier was calibrated as a function of the RF input power from the signal generator to allow the W-band power applied via the probe to be varied over several orders of magnitude. The power reaching the UTC was estimated by taking into account the probe loss data supplied by the manufacturer and measurements of the loss between the antennas.

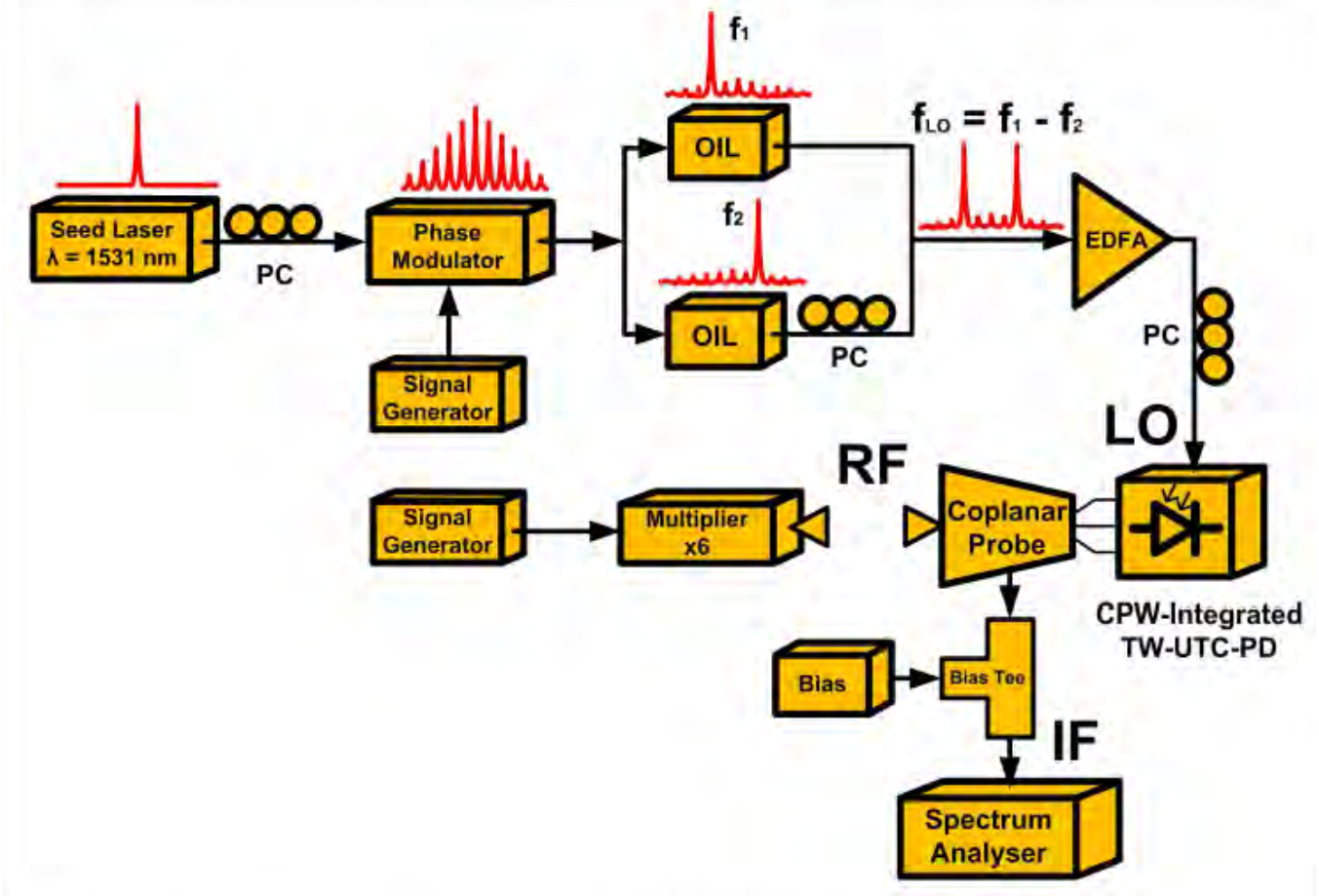

Figure 2: Experimental configuration for measurement of mixing gain of UTC optoelectronic mixer in W-band.

The optical LO was generated by heterodyning the outputs of two diode lasers which were optically injection locked to lines in an optical frequency comb generator consisting of a DFB laser (wavelength = 1550 nm) modulated using a lithium niobate phase modulator driven sinusoidally at 20 GHz. The comb lines to which the slave lasers were locked for the mixing experiments were separated by 100 GHz.

The IF signal was extracted from the internal bias port of the probe, while a separate bias tee was used to split the IF signal from the DC bias. The loss of this combination was calibrated in order to

allow the true IF power to be obtained. The minimum loss for the IF path was at 50 kHz, so the output of the multiplier was set to give this IF.

Some sub-harmonic mixing measurements were also made using a slightly modified experimental arrangement. In this case, the signal generator output was applied directly to the input of a DC – 67 GHz coplanar probe. This arrangement allowed the IF to be tuned over a wide frequency range.

Using a similar experimental arrangement to that shown in Figure 2, mixing in a packaged UTC-PD with integrated "bow-tie" antenna (Figure 3) was also studied. This enabled optoelectronic mixing to be investigated without the limitations imposed on the IF by the frequency response of the DC-bias port of the W-band coplanar probe with waveguide RF input. The integrated wide-band bow-tie antenna was designed to emit at frequencies in the range at 250 – 1500 GHz, so its performance was not optimised for W-band operation. The mm-wave signal was coupled into / out of the packaged UTC through a hemispherical silicon lens with a diameter of approximately 6 mm. An SMA RF connector mounted on the package was used to apply DC bias to the PD via a bond-wire connected to the integrated antenna. The SMA port was also used to extract the IF signal generated in these experiments, using an external bias tee to separate the DC bias and RF signals.

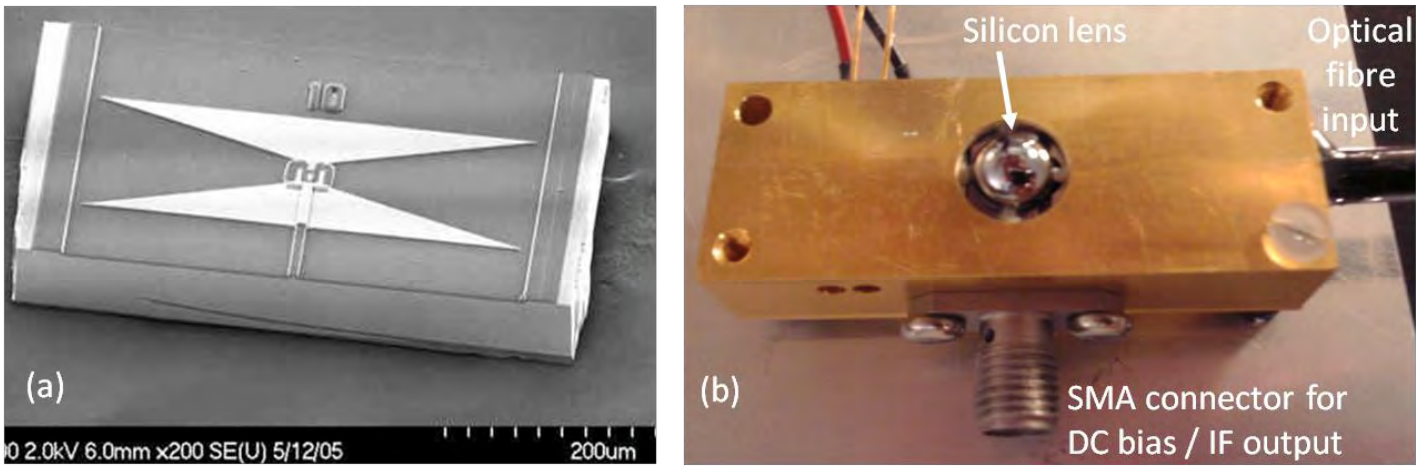

Figure 3: (a) SEM image of UTC-PD chip with integrated bow-tie antenna; (b) photograph of packaged UTC-PD.

4.2 Simulation of THz optoelectronic mixers

In order to understand the mixing mechanism behind the UTC optoelectronic mixer, an empirical model has been developed, based on the measured DC current-voltage (IV) characteristic of the UTC.

The effects of two separate non-linear phenomena in the device have investigated, initially independently, and then combined in a single simulation. The non-linear effects modelled are:

(1) The non-linearity associated with the dependence of the UTC differential conductance on the incident optical power.
(2) The non-linear terminal IV characteristics of the UTC.

The non-linear device capacitance, which varies with the terminal voltage, has been included as an additional non-linearity responsible for the mixing behaviour and to allow the frequency response of the UTC to be taken into account to some extent.

The modelling of the UTC optoelectronic mixing can be considered to consist of two key steps. The first step is to employ harmonic-balance techniques to analyse the UTC subjected to the large optical LO excitation alone without considering the small RF signal input. The second step is to analyse the

UTC mixer in a quasi-linear fashion in which the sole input to the mixer is the small electrical RF signal without considering the LO anymore. Frequency generation at the IF and other image frequencies are dealt with in the analysis using the concept of the conversion-matrix which is determined from the time-varying differential conductance of the nonlinear UTC in the model, which is derived from measured DC IV curves.

Figure 4 shows the model for the large signal part of the harmonic balance simulation.

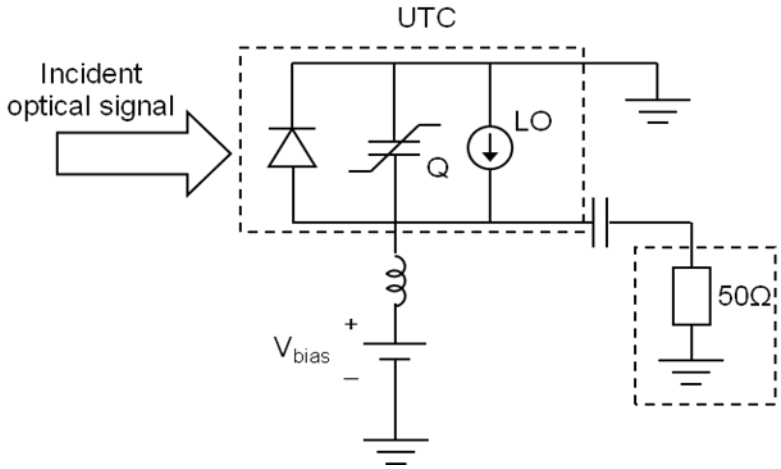

Figure 4: UTC large-signal model.

In Figure 4, the AC photocurrent due to the optical LO is represented by an AC current source in the UTC equivalent circuit model. The large signal terminal IV behaviour of the UTC is denoted by a diode symbol in Figure 4 and is mathematically generated by interpolating the measured IV data. The voltage dependent UTC capacitance is represented by Q. The reason for using the label "Q" instead of "C" is as follows. To model the non-linear UTC capacitance, it is not appropriate to insert simply a capacitor model whose capacitance varies with the terminal voltage in Figure 4, because the use of voltage dependent-capacitance is only applicable to small signal excitation. In our large signal model, it is therefore necessary to describe instead the amount of charge Q on the device capacitor with capacitance C. It is straightforward to find Q by integrating C with respect with V. It is assumed that the voltage dependence of the UTC capacitance follows that of a microwave Schottky barrier diode, i.e.

$$C(V) = \frac{dQ}{dV} = \frac{C_{j0}}{\left(1 - \frac{V}{\emptyset}\right)^{\gamma}}$$

In order to give the large variation in capacitance necessary to account for the experimentally observed change in photodiode bandwidth with bias voltage (see Section 5.1.2), the diffusion potential $\emptyset$ was set to 0.1 V, and the parameter γ, which determines the strength of the non-linearity, was assumed to be unity in our model. C_{j0} is the capacitance at zero bias voltage and a range of values have been used. It is trivial to show, by integration, that (for γ = 1):

$$Q(V) = -\emptyset C_{j0} \ln\left(1 - \frac{V}{\emptyset}\right)$$

The current flowing through the non-linear capacitor can be found in the time domain by differentiating the charge Q with respect to time. However, it is much easier to find the current at each harmonic in the frequency domain by multiplying each Fourier coefficient of the time-varying Q by $j2\pi f$ where f is the corresponding harmonic frequency. As described previously, the aim of the

large signal part of the harmonic balance simulation is to find the two time-varying nodal voltages in Figure 4. Once the large signal part analysis has been performed, the conversion matrices of the non-linear capacitance and conductance are calculated and used in the small signal analysis as shown in Figure 5, which also includes the input RF signal source.

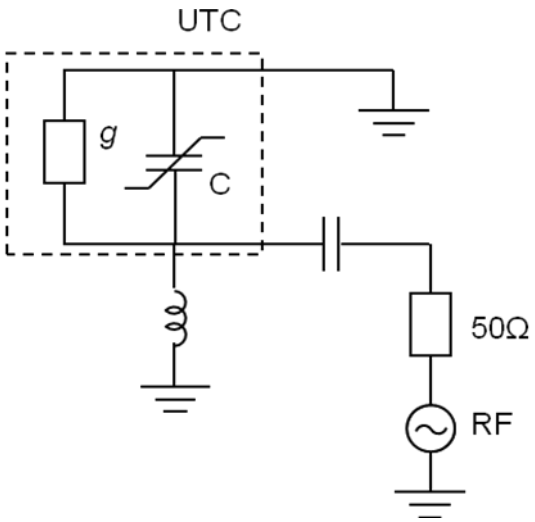

Figure 5: UTC small-signal model.

4.3 Data transmission over THz carrier

4.3.1 Data transmission using UTC down-converting mixer

Using a similar experimental arrangement to the W-band mixing experiment, wireless data transmission has been demonstrated using a UTC diode as a down-converting mixer. The experimental arrangement is shown in Figure 6. Binary phase shift keying (BPSK) modulation was applied to an 80 GHz carrier at a rate of 500 kb/s by phase modulating the output of the RF synthesiser used to drive the x6 frequency multiplier, and the signal radiated from a horn antenna with a nominal gain of 20 dBi. The signal was received after transmission over a few cm of air using an identical antenna and coupled to the UTC mixer using a coplanar probe. An optical LO was generated using an optical heterodyne method similar that described in Section 4.1, with the frequency chosen to give an IF of 5 MHz. The phase modulated IF was demodulated to baseband and displayed using a vector signal analyser.

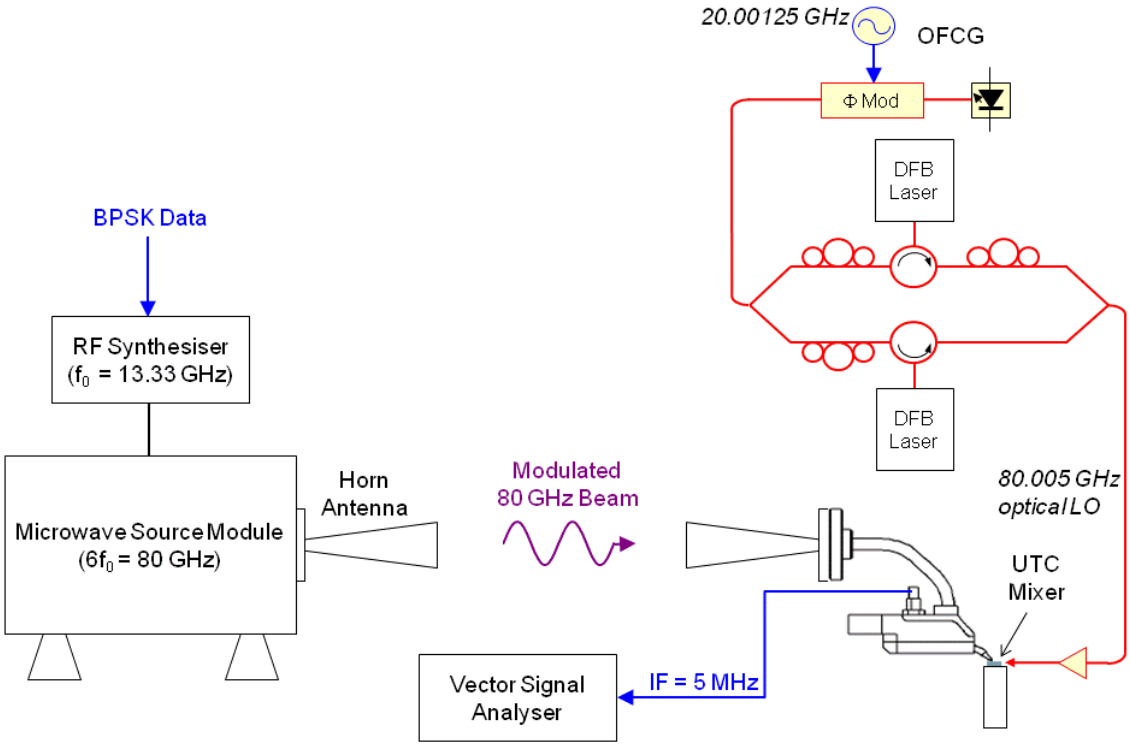

Figure 6: Experimental configuration for wireless data transmission in the W-band, using a UTC photodiode as a down-converting mixer.

4.3.2 Gb/s wireless data transmission using SBD mixer

Wireless data transmission was investigated using the experimental arrangement shown in Figure 7. An optical heterodyne signal was generated by combining the outputs of two free-running external cavity lasers (ECL1 and ECL2), the wavelengths of which were set to give a frequency difference of approximately 200 GHz. After optical amplification using an EDFA, the combined optical heterodyne signal was modulated with a 2^7-1 PRBS data pattern using on-off keying (OOK) at 1 Gb/s in a Mach-Zehnder electro-optic modulator. The resulting signal was re-amplified using a further EDFA and input to a packaged UTC PD similar to that shown in Figure 3b, although in this case the integrated wideband antenna was of a log-periodic design. Polarisation controllers (not shown in the diagram) were used to align the polarisation states of both ECLs to the modulator polarisation axis (and hence to each other), and to align the data-modulated signal to the optical waveguide of the UTC (so maximising the photocurrent generated). The optical input power to the UTC was +13 dBm (in the fibre) and resulted in a mean photocurrent of 2.0 mA at a reverse bias voltage of 2 V and temperature of 17°C. These operating conditions were chosen to minimise the risk of damage to the prototype UTC PD by excessive thermal dissipation, but result in a relatively low radiated power at 200 GHz. Significantly higher radiated power would be expected at higher reverse bias voltage (giving wider PD bandwidth) and photocurrent.

This arrangement generated an OOK modulated signal at 200 GHz, which was directed towards a receiver based on an electrically pumped Schottky barrier diode (SBD) sub-harmonic mixer from Virginia Diodes Inc. (type WR5.1SHM). The SBD is packaged with waveguide inputs for the G-band (140 – 220 GHz) signal (RF) and W-band (75 – 110 GHz) sub-harmonic local oscillator (LO). The LO was obtained from an RF signal generator using a x6 electronic multiplier. The frequency of the RF signal generator was set to give an intermediate frequency (IF) of 2.5 GHz. The SBD package was mounted directly on the waveguide output of the multiplier, and a G-band horn antenna (nominal gain 20 dBi) was mounted directly on the RF input of the mixer. The mixer assembly (multiplier, SBD, and horn antenna) was mounted on a translation stage, in order to allow the transmission distance to be

varied. The UTC was mounted on an x-y translation stage, which allowed adjustment of the UTC position in the plane orthogonal to the transmission link axis.

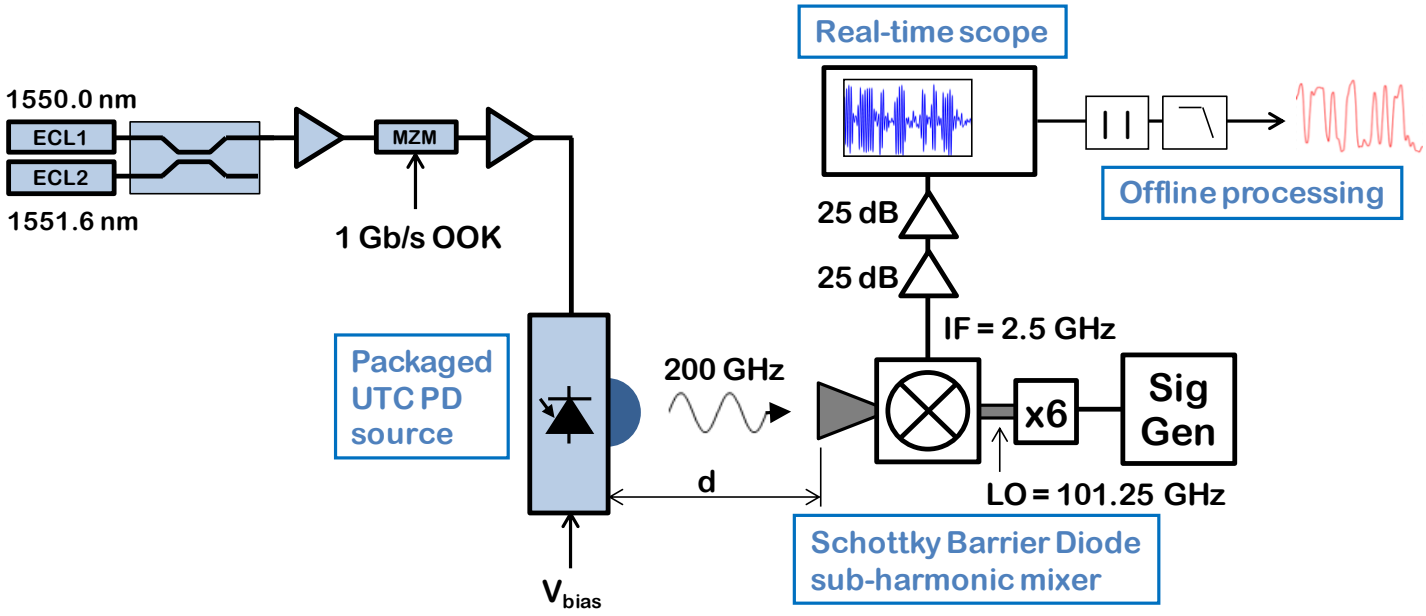

Figure 7: Experimental arrangement for wireless data transmission on 200 GHz carrier.

The IF output was taken from an SMA connector on the mixer package. The IF power was below -50 dBm, so two stages of electrical amplification were used to boost the IF signal to a suitable level for subsequent processing. The power of the amplified IF was measured using an electrical spectrum analyser, while a real-time scope was used to capture the modulated IF for subsequent off-line processing. The bandwidth of the real-time scope used was 3.5 GHz, which limited the IF and modulation rate in this experiment. The maximum sampling rate of the scope was 40 Gsamples/s, but for the results presented in Section 5.3.2 a sampling rate of 10 Gsample/s was used.

Since the frequency difference of the ECLs is not locked, the nominally 200 GHz carrier exhibited frequency instability and jitter, and hence synchronous detection could not be employed. Instead, the data were recovered by offline processing in MATLAB which mimics analogue envelope detection. The IF signal was first filtered in the frequency domain to remove low frequency spectral components (frequency jitter and amplitude variation) and to limit noise; an IF bandwidth of 2 GHz centred on 2.5 GHz was used. Then the IF was envelope detected by taking the absolute value of the filtered IF and applying a baseband filter (5^{th} order Bessel filter with 0.5 GHz -3 dB bandwidth), resulting in baseband data being recovered.

To estimate the bit error ratio (BER), a decision threshold was applied to the demodulated baseband data to obtain a binary value for each sample, which was compared to the corresponding value in the transmitted data sequence. The overall BER was calculated for each of the 10 samples per bit (1 Gb/s data was sampled at 10 Gsamples/s) to determine the optimum decision sample, and the decision threshold was varied to find the global minimum BER. Data sequences, each of 1 Msamples, were processed for several transmission distances to obtain the BER as a function of distance or received power. With this sequence length, BER can only be measured down to approximately 10^{-4} with any confidence (10 bits in error in a total of 10^5 bits). However, this allows the distance or received power for a BER of 10^{-3} to be estimated, which is sufficient for reliable transmission if forward error correction is employed.

5 RESULTS AND DISCUSSION

5.1 Optoelectronic mixing in UTC photodiodes

5.1.1 UTC photodiode chip with coplanar waveguide connection

Throughout the various stages of the project, optoelectronic mixing has been investigated in various UTC-PD samples, over a range of operating parameters (frequency, photocurrent, bias voltage). In this section, we present representative experimental results for optoelectronic mixing using a UTC-PD with dimensions 2 μm x 25 μm. These experiments were performed in Phase 3 of the project. Details of the epitaxial structure of the device are given in [2]. An optical heterodyne signal at 100 GHz ("optical LO") was coupled into the PD using a lensed optical fibre. With just the optical LO applied to the UTC-PD, an output power of 0 dBm was measured on an external 50 Ω load for a photocurrent of 10 mA and a reverse bias of 4 V. This is consistent with separate measurements of the frequency response of the UTC-PD, which gave a 3-dB bandwidth of 89 GHz and relative response at 100 GHz of -4 dB.

Figure 8 shows the measured DC photocurrent as a function of reverse bias and optical LO power in the lensed fibre (i.e. the IV characteristic). The maximum applied bias was restricted to 4 V to limit the maximum dissipated power and to avoid thermal failure. The PD shows a non-linear variation of photocurrent with optical power at high reverse bias (> 3 V), and rapidly increasing differential conductance (slope of photocurrent vs bias voltage) at higher optical powers. Both of these non-linearities are believed to enhance mixing in the UTC-PD.

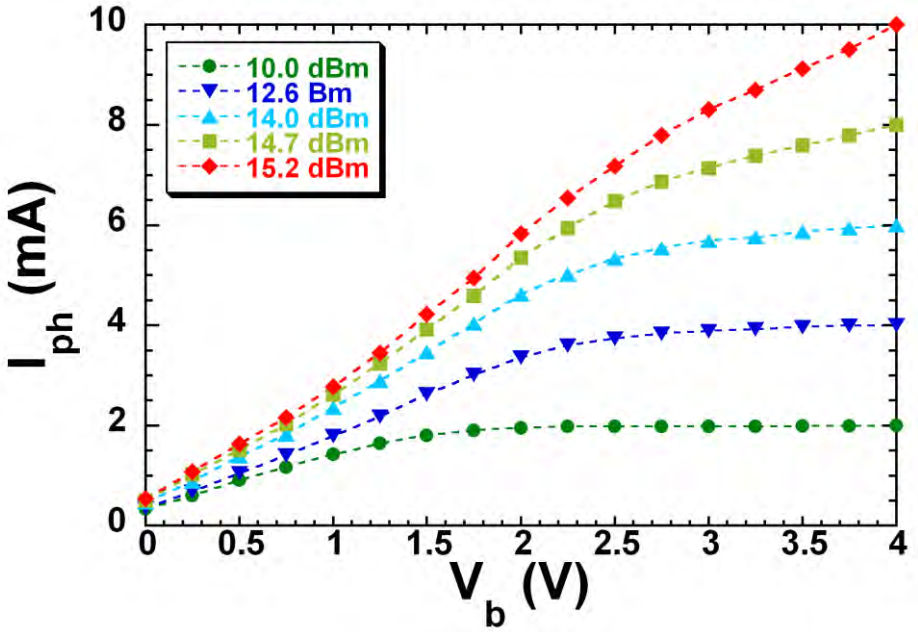

Figure 8: DC photocurrent as a function of reverse bias and optical LO power.

Figure 9 shows the conversion gain*, measured for the same conditions as Figure 8, for optoelectronic down conversion of a 100 GHz mm-wave signal to an IF of 50 kHz. The mm-wave signal was applied to the UTC-PD at a power of 0 dBm. The trends seen previously [3, 4, 5] were again observed. At lower optical power (10 dBm), the conversion gain was low (< -60 dB), and showed a maximum at 1 – 1.5 V reverse bias. As the optical power was increased, the conversion gain at higher reverse bias (> 2.5 V) increased dramatically, with the highest conversion gain (-32 dB) being obtained at the maximum applied optical power and bias voltage.

* We define the mixer conversion gain as the ratio of the measured IF power to the W-band carrier power applied via the coplanar probe.

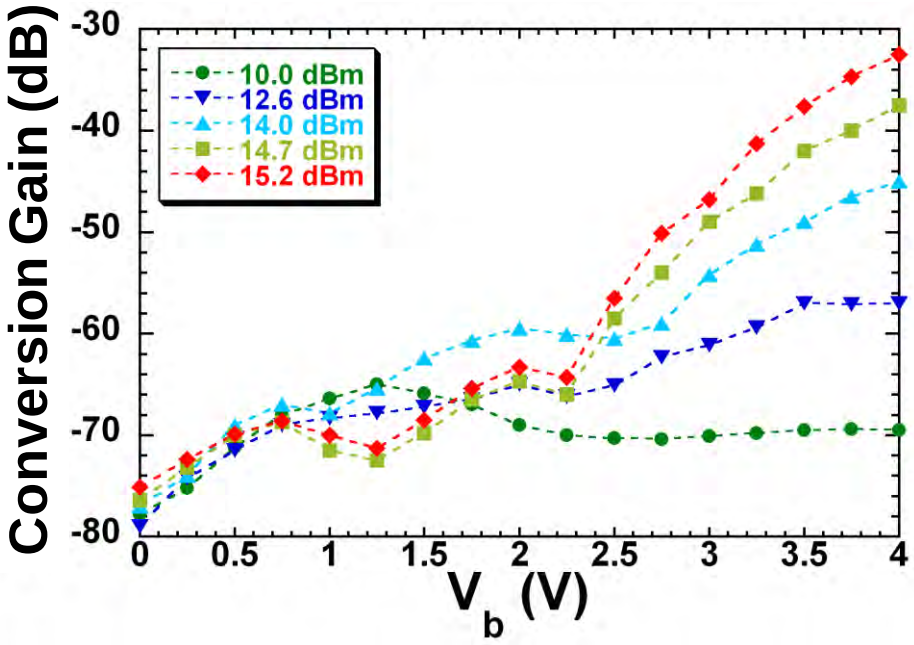

Figure 9: Conversion gain for fundamental mixing as a function of reverse bias and optical LO power.

The maximum conversion gain observed was an improvement of approximately 8 dB over the conversion gain we measured in Phase 2 on a 4 μm x 25 μm device from the same batch (Figure 19) [3, 4]. The variation with optical power of the photocurrent and differential conductance at 4 V bias were almost identical for the two UTC-PDs, so this improvement is attributed to operation at higher maximum DC photocurrent (10 mA, instead of 7 mA) and improved frequency response in the case of the latest device tested. Together, these gave an increase of 9 dB in mm-wave power generated by the optical LO. The improved frequency response of the latest UTC-PD tested may be due to reduced device capacitance because of its smaller size.

5.1.2 Explanation of the optoelectronic mixing mechanism

The mixing process is believed to be largely due to non-linearities in the PD responsivity and differential conductance as the optical power and the bias voltage are varied (as noted above for the IV plot of Figure 8), and is illustrated schematically in Figure 10. If we assume that the RF signal causes a small-signal variation of the bias voltage, then a corresponding variation of the PD photocurrent will occur, the magnitude of which will depend on the differential conductance at the PD operating point. Applying a modulated optical LO changes the PD operating point at the LO frequency, causing the differential conductance, and hence the RF photocurrent, to be modulated. This modulation corresponds to mixing of the RF and LO waves, giving an IF at their difference frequency.

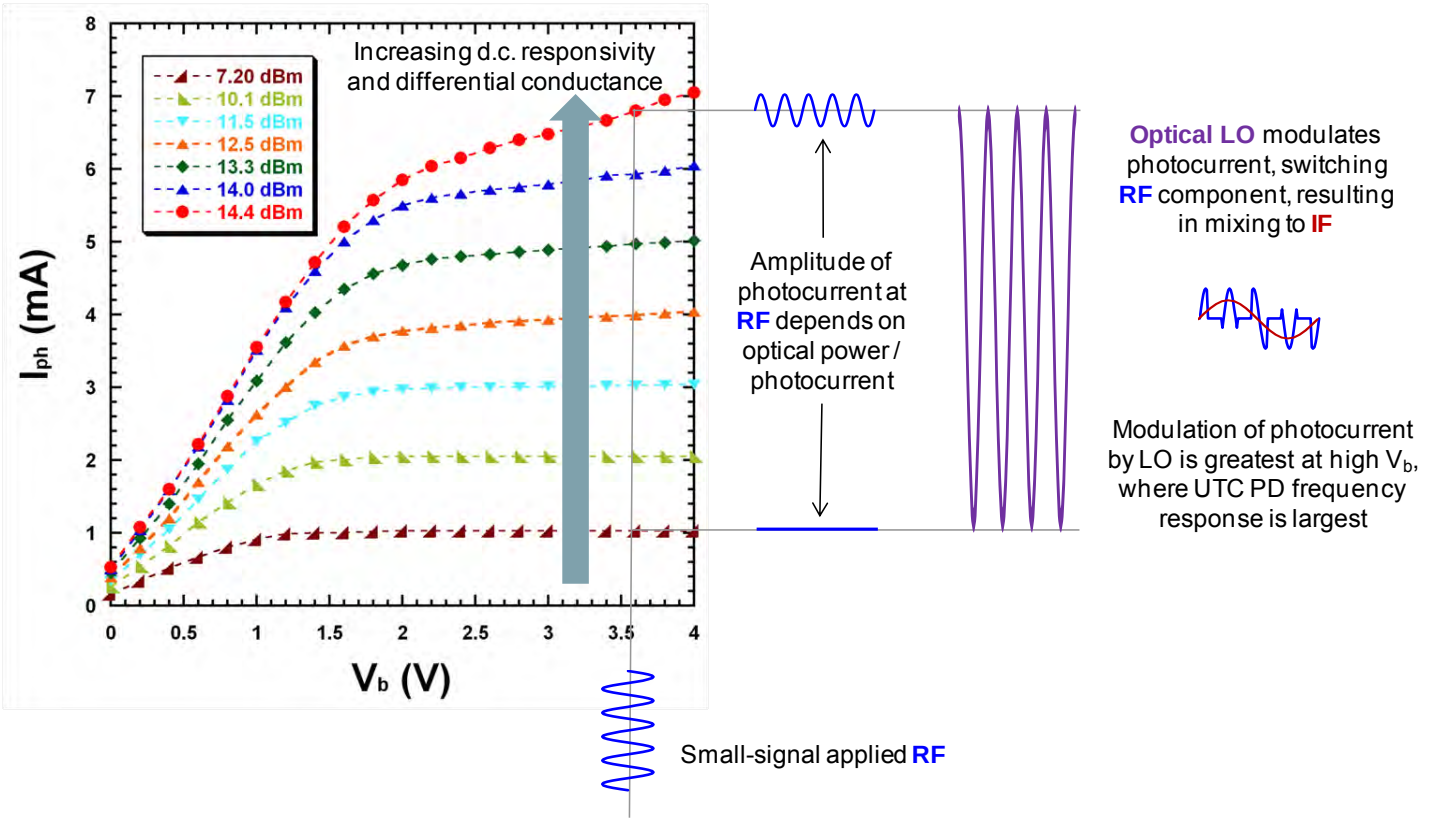

Figure 10: Diagrammatic illustration of optoelectronic mixing in a UTC-PD.

From the DC IV characteristic it appears that changes in differential conductance occur at all bias voltages when the optical power is varied. However, the frequency response of the photodiode must also be taken into account, and this is greatly reduced at low bias voltages, as illustrated by the example response shown in Figure 11. At frequencies of 100 GHz or above, the bias voltage should typically be greater than 2 V if the response is not to be seriously impaired, and a bias voltage of 3 or 4 V is preferred. At these higher bias voltages, significant non-linearity in the responsivity and differential conductance is only observed at high photocurrents (optical powers). Hence the mixer gain is maximised by operating at high bias voltages (giving large frequency response) and high photocurrents (giving significant non-linearity).

As discussed in Section 4.2, it should be noted that the LO modulates the PD operating point by two mechanisms. First, the variation of optical power through the LO cycle modulates the photocurrent, as just described. Second, the photocurrent generated by the LO will flow through the load impedance and thus will modulate the bias voltage at the LO frequency. If the LO frequency is low enough for the photocurrent to follow the DC characteristics of Figure 10, a peak-to-peak variation of the photocurrent of up to 15 mA might be generated for a mean optical power of 14 dBm (assuming 100% modulation depth of the optical LO), giving a bias voltage modulation of 0.75 V p-p with a 50 Ω load. However, for a LO frequency in the W-band, the voltage modulation will be reduced because of the reduced frequency response of the PD. Experimentally, the detected electrical power at an LO frequency of 100 GHz was -9 dBm for the UTC-PD with the characteristics shown in Figure 10, corresponding to 0.225 V p-p across a 50 Ω load. At bias voltages close to 4 V, variations of bias voltage of 1 V p-p or less do not change the differential conductance significantly at constant optical power. Therefore, for higher bias voltages (>2.5 V), we expect the dominant mixing mechanism to be related to the change in differential conductance with photocurrent. However, for bias voltages in the vicinity of the „knee" in the IV curves (i.e. 1 – 2 V), the modulation of the bias voltage in response to the LO will also be important, and may be the dominant mixing mechanism.

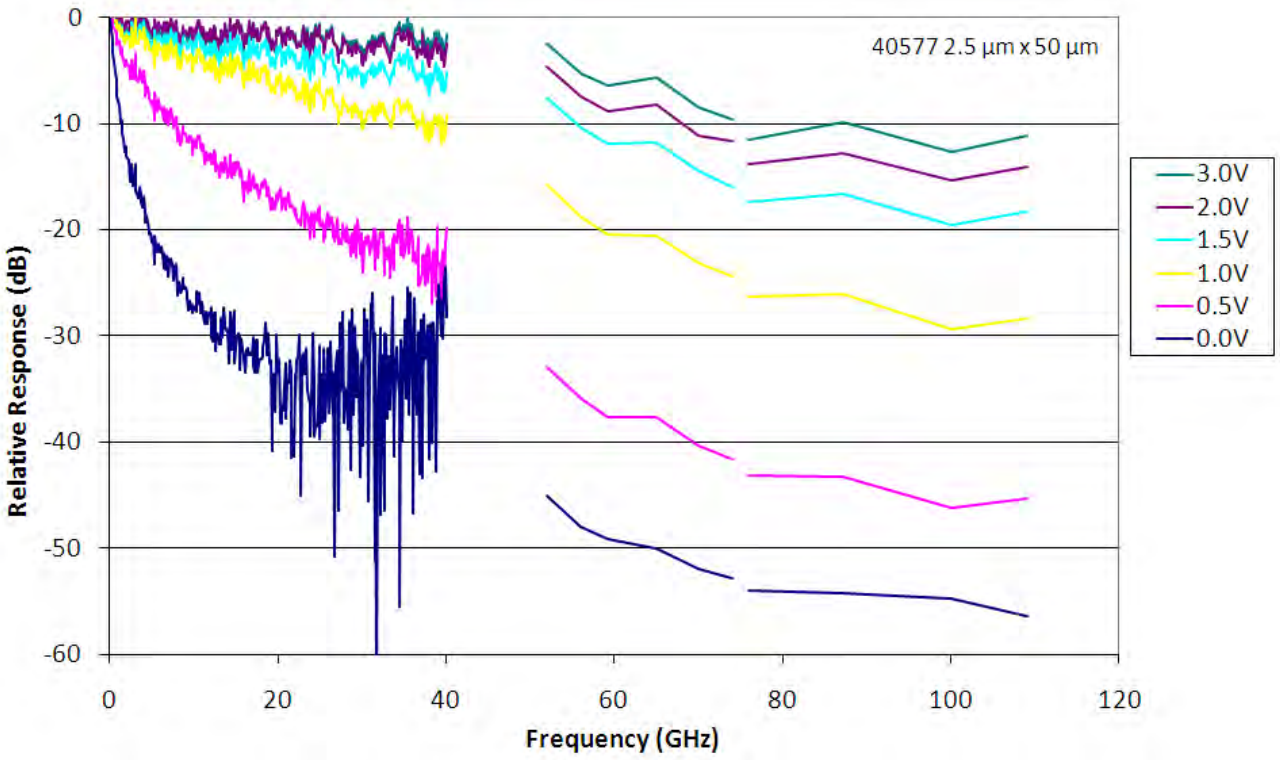

Figure 11: Relative frequency response of UTC as a function of optical modulation frequency.

We can thus describe qualitatively the mixing performance shown in Figure 9 by reference to Figure 8 and Figure 11, as follows. At low reverse bias, <1 V, the poor frequency response at 100 GHz means that there is very little modulation of the properties of the UTC at any optical input power, and hence the IF power is very low under all conditions. At intermediate reverse bias, in the vicinity of the knee in the IV curve (1 – 2 V), it is likely that both modulation of the bias voltage and the differential conductance play a role. A peak in the IF power is observed close to the voltage of the knee, which increases with increasing optical power. The frequency response is improved in this range of bias voltages, but is still quite low at 100 GHz, so the conversion gain remains low (< -60 dB). At higher reverse bias, > 2.5 V, the mixing performance is dominated by modulation of the differential conductance in response to the change of optical power in the LO, and consequently is highly dependent on the mean optical power, since the differential conductance under DC conditions increases very non-linearly with optical power. At these reverse bias voltages, the frequency response at 100 GHz is improved, but is still considerably reduced compared to low frequency. Consequently, the modulation of the differential conductance, and conversion gain, is not as large as would be inferred from the DC IV curves.

The fact that the mixing performance can be related to the DC IV curves suggests that the physical mechanism determining the DC performance at high photocurrent and bias voltage is a high-speed effect (rather than, say, a thermal effect). In addition, the highly non-linear increase in the differential conductance with optical power suggests that the mechanism is related to the density of photo-generated carriers, perhaps resulting from the accumulated charge modifying the band structure of the device. This suggestion is supported by the observation that the UTC which shows the largest differential conductance at high photocurrent and bias voltage of those tested so far also has the smallest physical dimensions (hence the largest density of photo-generated carriers for a given photocurrent).

5.1.3 IF linearity and sub-harmonic mixing experiments

The dependence of the IF power on the RF signal power was investigated for the UTC-PD giving the conversion gain results shown in Figure 9. Results are shown in Figure 12 for reverse bias of 4 V and DC photocurrent of 10 mA. For fundamental mixing, as discussed so far, a linear relation between the RF and the IF powers was obtained over more than five decades of power variation. This is important, as it means that down conversion to the IF of amplitude modulation on the RF signal will be achieved without distortion. IF power as high as -28 dBm was obtained.

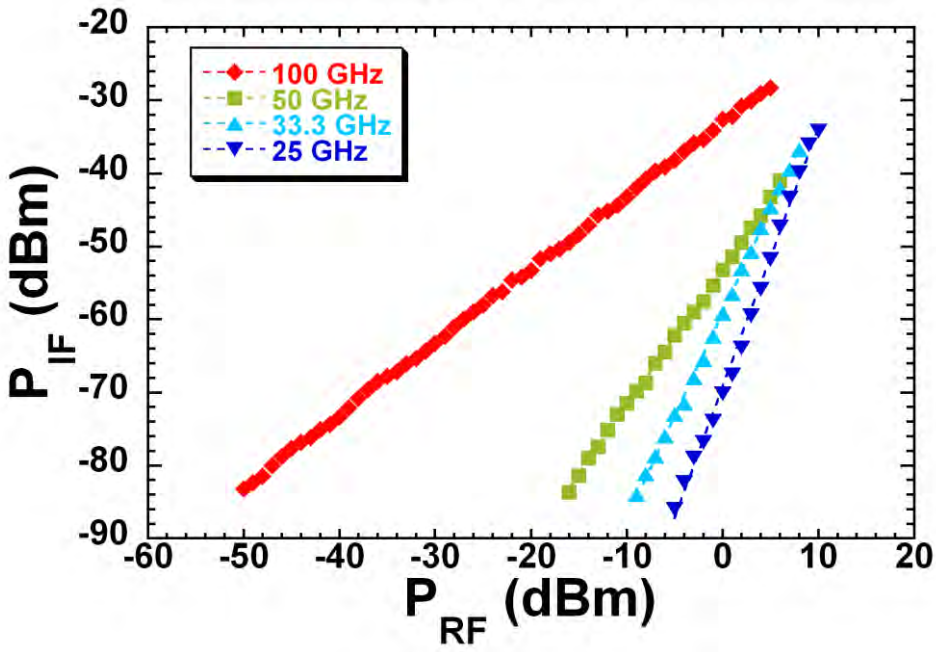

Figure 12: IF power as a function of RF power for fundamental and harmonic mixing. (The legend shows the frequency of the applied RF signal.)

Figure 12 also shows equivalent results for sub-harmonic mixing, where the RF signal is applied at a sub-multiple of the optical heterodyne signal. Results are shown for 2nd, 3rd and 4th harmonic mixing, using RF signals of approximately 50, 33 and 25 GHz respectively (the exact frequencies were chosen to give an IF of 50 MHz). For sub-harmonic mixing, the IF power is found to vary as $(P_{RF})^m$, where m was 1.98, 3.02 and 3.87 for 2nd, 3rd and 4th harmonic mixing.

This form of sub-harmonic mixing is not of interest for down conversion of data-modulated RF signals, but could be of use for frequency and phase locking an optical heterodyne to a relatively low-frequency RF sub-harmonic reference. The sub-harmonic mixing experiment has also enabled the IF bandwidth of the UTC-PD optoelectronic mixer to be investigated (the experimental arrangement for fundamental mixing severely restricts the IF frequency that can be used). Using first-harmonic mixing, the IF was varied over a wide range by changing the applied RF frequency at 10 mA photocurrent and a reverse bias of 4 V. The conversion gain, relative to the maximum value of -50 dB obtained for an IF of 19 GHz, is shown in Figure 13. The conversion gain was found to be relatively flat (<6 dB variation) for IFs from 5 GHz to 23 GHz, indicating that the UTC-PD could be used for down converting multi-Gb/s data signals. The large reduction in conversion gain for IF less than 5 GHz is thought to be associated with high impedance of the UTC at these frequencies, as observed in S_{11} measurements, leading to mismatch with the external circuit.

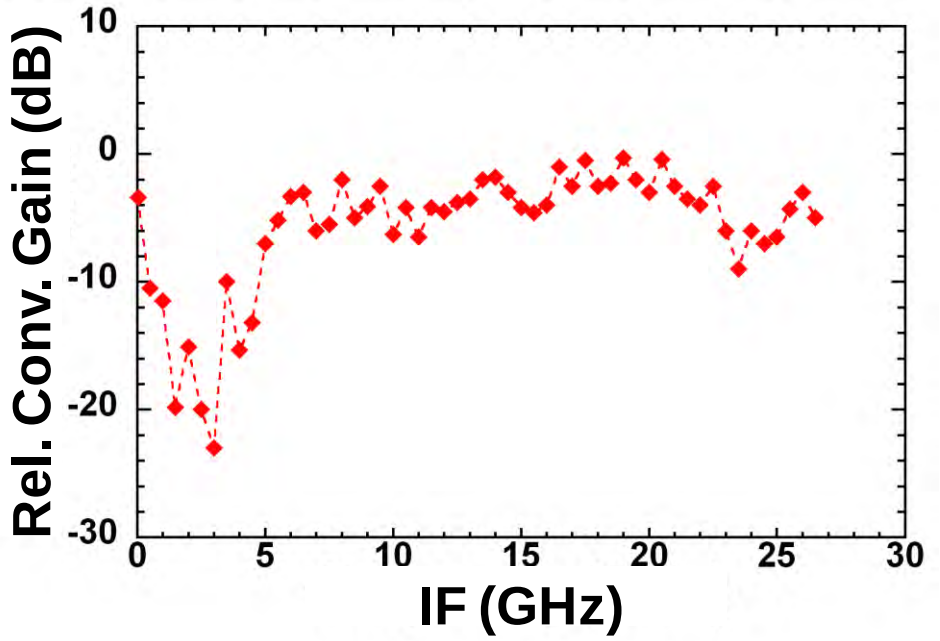

Figure 13: Relative conversion gain as a function of IF frequency.

We have also investigated sub-harmonic mixing where the frequency of the *optical LO* is at a sub harmonic of the mm-wave signal to be down converted. This might simplify the optical heterodyne generation scheme for the optical local oscillator, since a narrower optical comb source could be used. A comparison of fundamental and sub-harmonic mixing of this type is shown in Figure 14. The legend shows the frequency of the optical LO and the RF power generated by the UTC-PD when only the optical LO is applied. It can be seen that significantly more power is generated at the lower frequency, to some extent compensating for the lower conversion gain with sub-harmonic mixing. The variation of IF power with reverse bias voltage is similar for both fundamental and first-harmonic mixing, but the IF power is typically 13 dB lower for the sub-harmonic mixing.

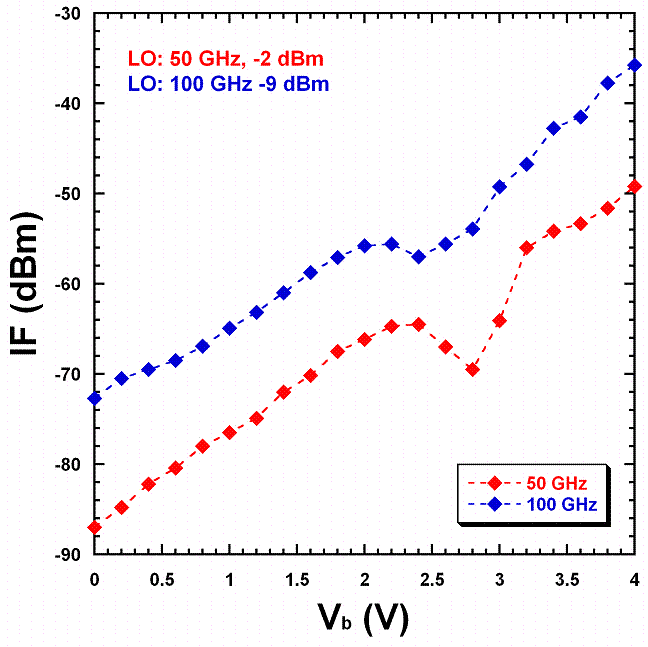

Figure 14: Variation of IF power with reverse bias voltage for fundamental and sub-harmonic optical LO frequencies.

5.1.4 Packaged UTC photodiode with integrated bow-tie antenna

The mixing performance of the packaged UTC-PD was first investigated as a function of IF. The LO signal was an optical heterodyne at a frequency of 80 GHz and power of 17 dBm. To avoid the risk of damaging the PD, the reverse bias was limited to 1.5 V. The conversion gain showed a weak maximum for a reverse bias of around 1 V, so this voltage was used for subsequent measurements. Under these conditions, the mean photocurrent was 2.5 mA and the power generated at 80 GHz was -21 dBm. A CW electrical signal at frequencies in the range 81 GHz to 90 GHz and a power of approximately 4 dBm was applied to the UTC-PD using a x6 multiplier W-band source and a 20 dBi horn antenna. The detected IF power as a function of IF frequency is shown in Figure 15. The conversion gain of less than -65 dB is consistent with measurements on unpackaged UTC-PDs at similar photocurrent and reverse bias.

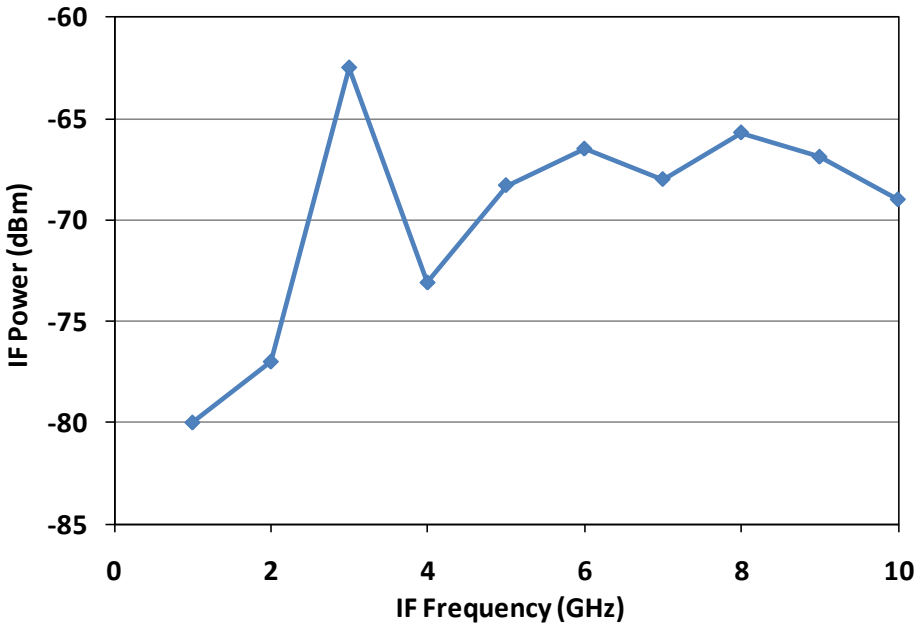

Figure 15: Variation of IF power with IF frequency for down conversion from 80 GHz using packaged UTC-PD mixer.

For IFs in the range 5 to 10 GHz, the detected IF power varies by less than 3 dB, demonstrating that the UTC mixer would be suitable for down converting wide-bandwidth mm-wave data signals to an IF in the RF band. For IF below 5 GHz, the IF power generally reduces, apart from at 3 GHz, where there is a strong peak. Both effects might be related to changes in the PD resistance altering the matching to the external load (see also Section 5.1.1).

The packaged UTC mixer was then investigated with a photonic heterodyne source in place of the multiplier source, using an unpackaged UTC with coplanar waveguide electrical connection to generate the incident mm-wave signal. The transmitter UTC-PD output was coupled to a horn antenna (20 dBi) using a W-band coplanar probe with waveguide output. The heterodyne source generated -2 dBm at 80 GHz, at a mean photocurrent of 9.6 mA. The optical LO heterodyne system was operated at 77 GHz in this experiment, to give an IF of 3 GHz.

The IF power was recorded as a function of the distance between the horn antenna and the packaged UTC, as shown in Figure 16. A trendline proportional to $1/(d+d_0)^2$ has been added, where d is the measured distance from the transmitter, and d_0 accounts for the virtual image position of the source, resulting from the use of the silicon lens. The value of d_0 is chosen as 1.55 cm to give a good fit to the data.

Using the Friis transmission equation, and assuming the IF power is proportional to the RF power, we can write:

$$P_{IF} = P_R - G_m = (P_T - G_m) + G_T + G_R - 20\log_{10}(4\pi\, d / \lambda)$$

where P_T is the transmitter power (in dBm), G_m is the mixer conversion gain (in dB), G_T, G_R are the transmitter and receiver antenna gains (in dB), and λ is the wavelength of the carrier. The fit gives:

$$(P_T - G_m) + G_T + G_R = -45\,\text{dBm}$$

Assuming $P_T - G_m$ = -77 dBm (the measured IF power for d = 0), and G_T = 20 dB (the nominal value for the horn antenna), we can estimate G_R to be approximately 12 dB.

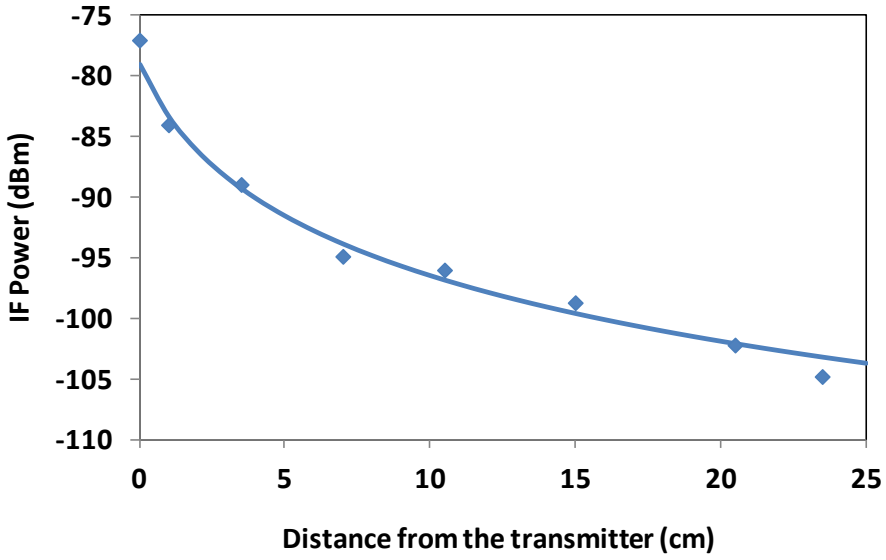

Figure 16: Variation of IF power with distance using packaged UTC-PD optoelectronic mixer.

5.2 Simulation of THz optoelectronic mixers

As an example of the simulation approach, we show results obtained using the DC IV curves shown in Figure 10. The differential conductance as a function of bias voltage and optical power was estimated at the measurement points, and interpolation was used within the model to obtain the differential conductance at intermediate values. The following additional parameters were used:

RF: 100 GHz + 2 MHz (as electrical input to the UTC)
Optical LO: 11.4 dBm mean optical power, 100% modulation index at 100 GHz
IF: 2 MHz (mixed output of the UTC optoelectronic mixer)

Figure 17 shows the simulated detected LO electrical power versus the reverse bias voltage for zero-bias capacitance values of 1 fF and 2000 fF. The former value gives negligible reduction of the photodiode response at 100 GHz in a system with 50 Ω load impedance, so corresponds to the performance expected at low RF and LO frequencies. With negligible capacitance, the detected LO electrical power is lower at low reverse bias because the mean photocurrent is lower (c.f. Figure 10). The larger value of capacitance was chosen from several modelled as it gives a similar reduction in response at ~4 V reverse bias to that observed experimentally (~10 dB simulated reduction, compared to 8 dB measured). In this case, the increased capacitance at low reverse bias results in greatly reduced response at 100 GHz; for instance, at 1 V reverse bias the response relative to the

predicted low-frequency response (C_{j0} = 1 fF) is -20 dB†. The simulated detected power is always less than -15 dBm, so the bias voltage modulation generated is less than 0.11 V p-p. Hence mixing due to the voltage-dependent non-linearity is expected to be small compared to the modulation of the differential conductance by the optical variation, at least at high bias voltage.

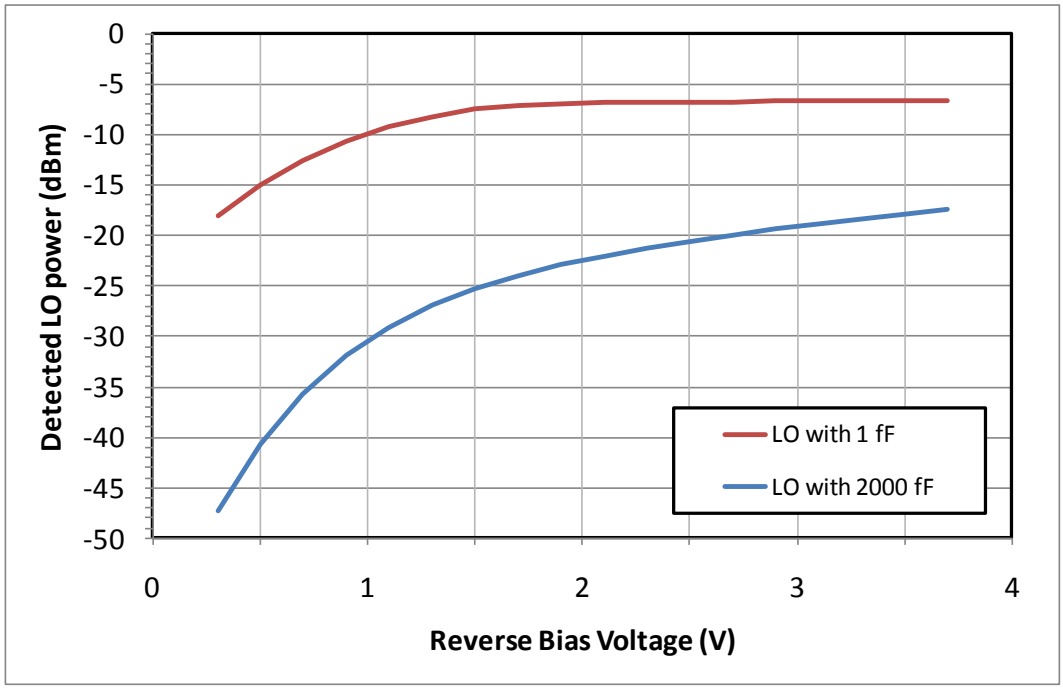

Figure 17: Simulated detected LO power vs reverse bias voltage for different zero-bias capacitance values.

Figure 18 shows the simulated conversion gain versus reverse bias voltage for the same two values of zero-bias capacitance, C_{j0}. Comparing the two curves in this figure, we see that the increased capacitance at low reverse bias voltages greatly reduces the conversion gain at these voltages. The capacitance shunts some of the photo-generated LO current, reducing the induced LO voltage variation driving the voltage-dependent non-linearity, and also some of the applied RF, so a reduced RF current flows through the time-varying conductance which is the main mechanism of the mixing process. The combined effect is a reduction in the conversion gain at high frequencies.

With the zero-bias capacitance set to 2000 fF, the variation of conversion gain with bias voltage shows the trends observed experimentally (compare with the result for mean optical power = 11.5 dBm in Figure 19). The conversion gain initially increases with bias voltage, reaching a maximum at around 1.3 V, then falls, before finally increasing again at high reverse bias. The simulated conversion gain at 3.7 V reverse bias is approximately -55 dB, in close agreement with the measured value for the same mean optical power. At lower reverse bias voltages, the magnitude of the simulated conversion gain is several dB higher than that measured, indicating that the experimental photodiode response reduces more rapidly than our voltage-dependent capacitance model predicts.

† It is worth noting, however, that the frequency response measurements in **Error! Reference source not found.** show a relative response of approximately -30 dB at 1 V reverse bias.

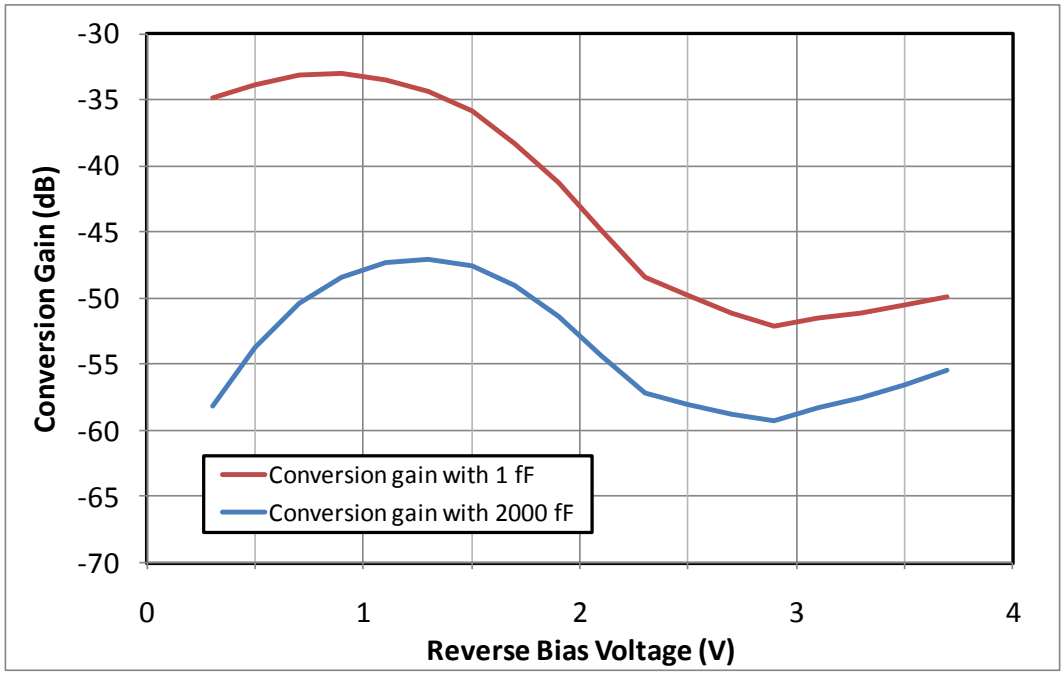

Figure 18: Simulated conversion gain vs reverse bias voltage for different zero-bias capacitance values.

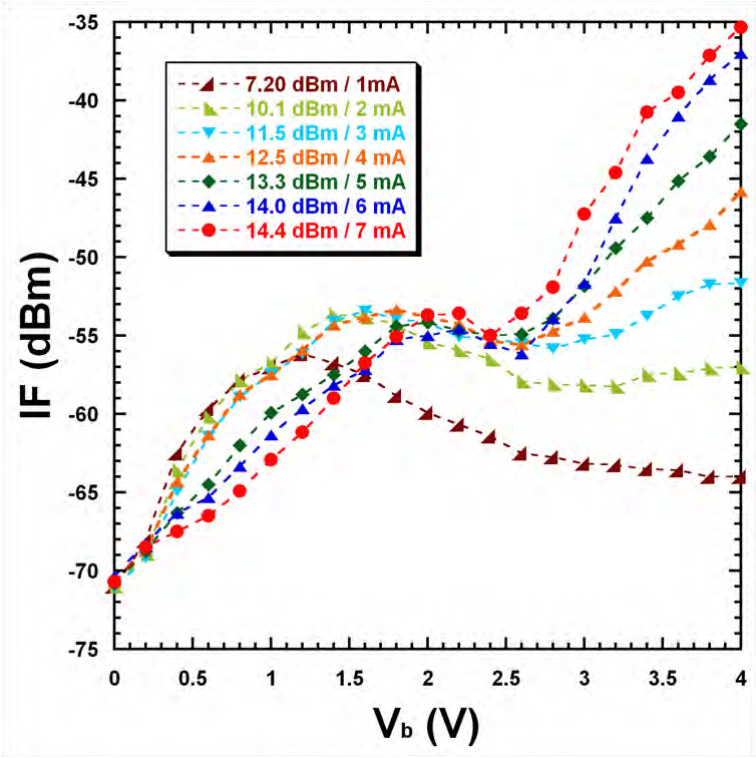

Figure 19: Measured conversion gain corresponding to IV characteristic in Figure 10.

It is also observed that the reduction in the conversion gain is always smaller than the corresponding reduction in the detected LO power. For example, at 0.5 V bias, the reduction in the conversion gain when the zero-bias capacitance is changed from 1 fF to 2000 fF is 19.8 dB while the corresponding reduction in the detected LO power is 25.6 dB. Similarly at 3.5 V reverse bias, the reduction in the conversion gain is 6.0 dB while the detected LO power reduces by 11.2 dB. This implies that the UTC behaves more like a switch than an analogue multiplier, a consequence of the highly non-linear variation of differential conductance with photocurrent.

5.3 Data transmission over THz carrier

5.3.1 Data transmission using UTC down-converting mixer

Example results for wireless BPSK transmission on an 80 GHz carrier, using a UTC optoelectronic mixer for down-conversion, are shown in Figure 20. The antenna separation was 5 cm. In this experiment, the transmission distance and data rate were limited mainly by the mixer conversion gain, which was approximately -74 dB for the UTC photodiode, LO optical power and bias voltage used. The IF power was approximately -70 dBm.

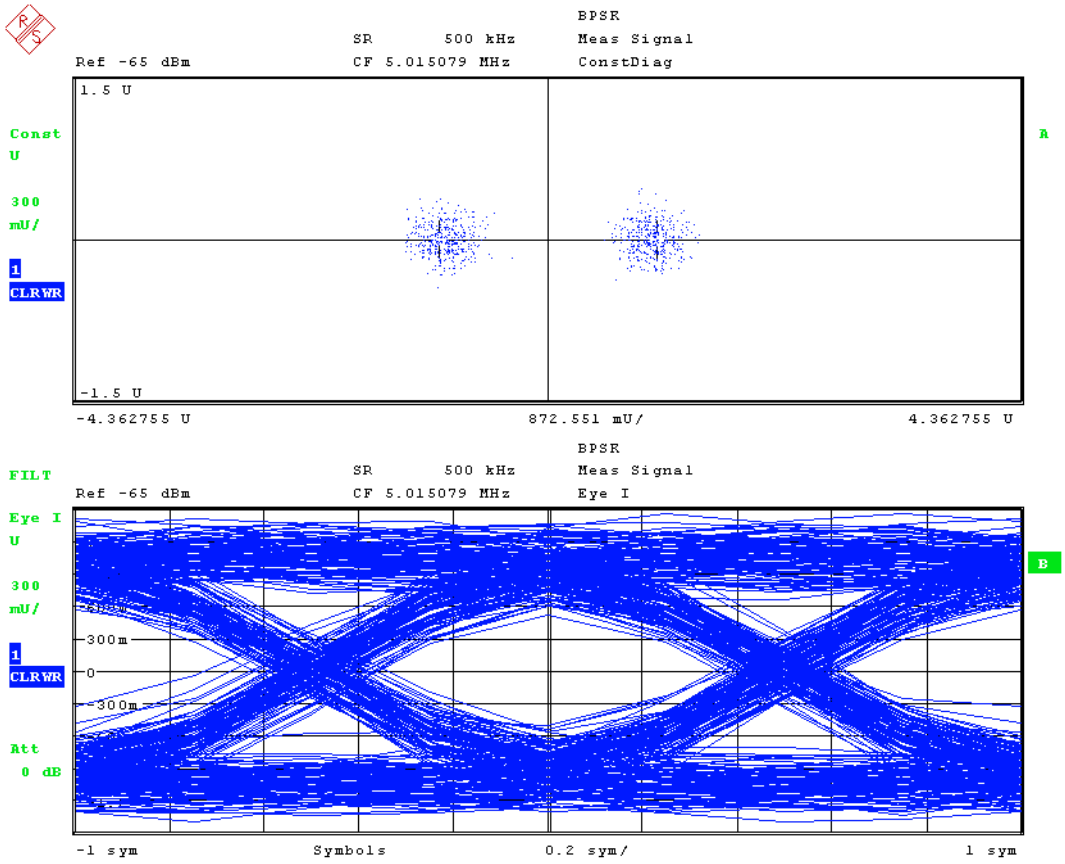

Figure 20: Received 500 kb/s BPSK constellation and eye diagrams from 80 GHz communication link using heterodyne receiver.

5.3.2 Gb/s wireless data transmission using SBD mixer

Figure 21 shows the unmodulated carrier power at 200 GHz received at the RF port of the SBD mixer for various distances between the UTC PD source and the front of the horn antenna (the distance shown as „d" in Figure 7). The carrier power has been estimated from the power measured after the IF amplifiers, assuming a total of 50 dB IF gain and a mixer double sideband (DSB) conversion gain of -6 dB (obtained from the manufacturer's data for the device used). It can be observed that the power variation with distance is closer to 1/d than the $1/d^2$ that might be expected. This is because the focusing action of the silicon lens in the UTC package produces a virtual image of the source some distance behind the front of the UTC package. Plotting the power against $1/(d+d_0)^2$ allows the virtual source location to be estimated as d_0 = 17.4 mm behind the front of the UTC package, and the equivalent isotropic radiated power (EIRP) to be -20 dBm. Using these values, we obtain the fit to the data shown by the dashed line in Figure 21.

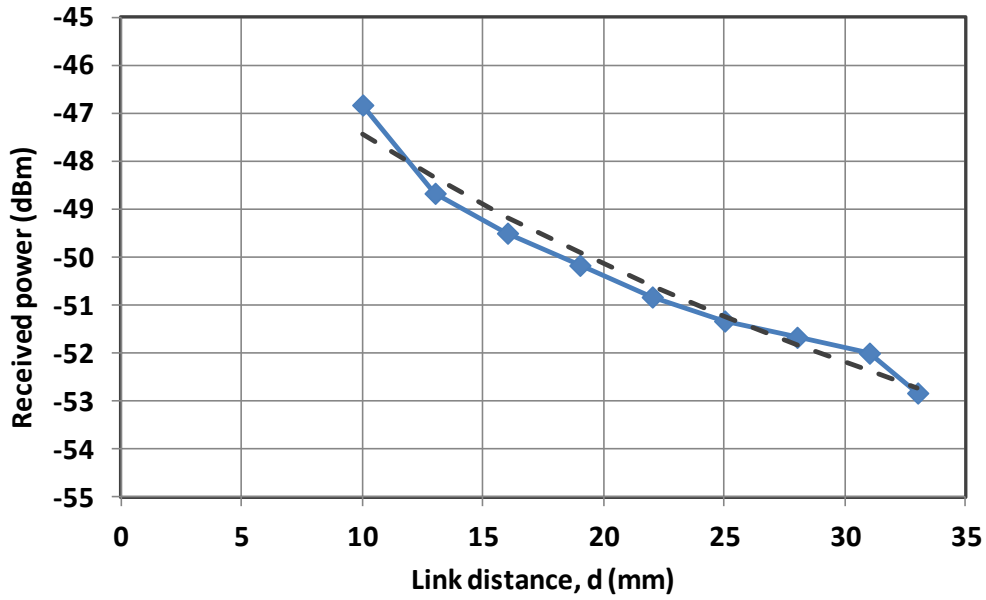

Figure 21: Received power of unmodulated 200 GHz carrier as a function of link distance (diamonds and solid line). The dashed line shows a fit, as explained in the text.

An example eye diagram for envelope-detected baseband data obtained by offline processing of the IF signal recorded by the real-time scope is shown in Figure 22. The link distance was d = 10 mm; for clarity only 1000 bits (10 ksamples) have been processed to obtain this image. It can be seen that the eye is clearly open.

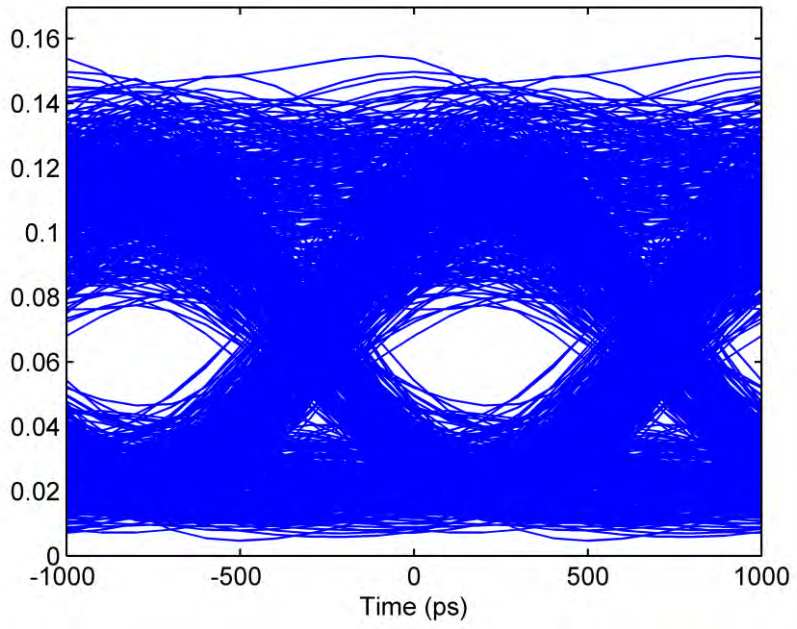

Figure 22: Eye diagram for 10 mm link distance, obtained by offline processing.

Processing larger datasets (100 kbits; 1 Msamples) obtained at a range of link distances (d = 10 mm to d = 33 mm) gives the BER results shown in Figure 23. Two horizontal scales are shown, carrier-to-noise ratio (CNR) and estimated received power at 200 GHz. The CNR is calculated from the power in the IF in ONES bit slots and the measured noise power in a 1 GHz bandwidth after the IF amplifiers. The dashed line shows the expected performance for envelope detection [6]. The discrepancy of about 2 dB at a BER of 10^{-3} is attributed to the imperfect envelope detection and more complex noise filtering in the experimental case; further analysis or simulation will be required to make a more realistic estimate of the theoretical performance.

The top horizontal scale in Figure 23 shows an estimate of the mean received modulated signal power at 200 GHz, assuming, as before, IF gain of 50 dB and DSB mixer conversion gain of -6 dB. The receiver sensitivity for BER = 10^{-3} is approximately -52 dBm (the corresponding link distance, d, is approximately 25 mm).

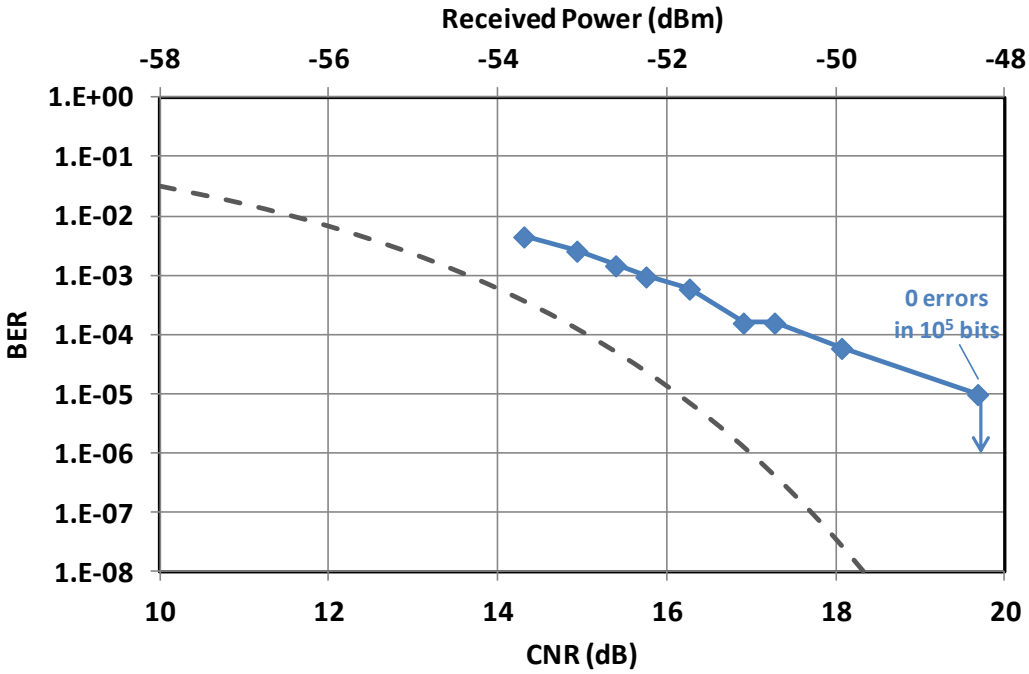

Figure 23: BER vs CNR / received power; the received power was varied by changing the link distance.

The link data rate is primarily limited by the source power, which with the receiver noise figure and bandwidth determines the CNR. Other elements of the experiment would allow the bit rate to be increased considerably with relative ease; for instance the electro-optic modulator used to apply modulation to the optical signal can operate at 10 Gb/s, while the offline detection scheme is limited by the analogue bandwidth of the real-time scope (similar scopes with bandwidth up to 33 GHz are available, approximately 10 times that of the scope used). In principle, therefore, the experiment could readily be extended to the target rate of 10 Gb/s, provided a suitable source with at least 10 dB higher output power were available.

6 FUTURE WORK

6.1 10 Gb/s transmission on 300 GHz carrier

Using the measured link performance at 1 Gb/s on a 200 GHz carrier, we can estimate the link characteristics of a system operating at the nominal project target data rate of 10 Gb/s, assuming the carrier frequency is 300 GHz.

Source power is one of the most critical parameters. A review of international research on the power generated using UTC-PDs at mm-wave and THz frequencies indicates that the power from such sources is unlikely to exceed 0 dBm at 300 GHz in the short to medium term [1]. Note that this is the same power obtained at 100 GHz from the UTC-PD used for the mixer experiments in Section 5.1.1, while in other experiments we have achieved output power as high as 10 dBm at 110 GHz [7]. However, the power is found to drop rapidly with frequency (at approximately $1/f^4$), so achieving 0 dBm at 300 GHz presents a significant challenge, although integrating resonant antennas can boost output over a particular band of frequencies. In the longer term, arrays of UTC-PDs may allow even higher power sources to be realised.

Using the parameters in Table 1, we find that the maximum link distance for a 10 Gb/s system with a source power of 0 dBm is 1 m. Provided the source power can be achieved, the results demonstrated in this project indicate that this link perfomance should be attainable. An increase in distance could be achieved by increasing the total antenna gain. For example, a link length of 10 m should be achievable with a total antenna gain (Tx + Rx) of 60 dBi, but with increased pointing accuracy being required.

Carrier frequency	300 GHz
Source power	0 dBm
Tx antenna gain	20 dBi
Rx antenna gain	20 dBi
Modulation / detection scheme	OOK / IF envelope
Bit rate	10 Gb/s
Received power / BER	-42 dBm / 10^{-3}
Mixer gain	-6 dB DSB

Table 1: Link parameters for 10 Gb/s transmission over 1 m at 300 GHz carrier frequency

6.2 Transceiver architectures and modulation formats

Figure 24 shows a number of possible transmitter and receiver options for THz communications systems. In Section 5.3.2 we used the combination of “Free-running lasers” and “SBD mixer / multiplier LO”, using envelope detection of the IF because it is tolerant of frequency instability and phase noise, which are poor when the optical heterodyne sources are not locked together. In Section 5.3.1, the “UTC OE mixer” receiver option was demonstrated, albeit with much lower mixer gain than we have subsequently shown the UTC-PD to be capable of. The “SBD envelope detection” scheme is not practical at the low received powers typical of systems with very high free-space path loss.

Future work will investigate the use of optical heterodyne LO generation, and compare its performance to the multiplier LO approach; in the longer term, photonic integration of the optical heterodyne generation (OHG) should allow much more compact transceivers to be developed.

Using “Phase locked lasers” in conjunction with the existing “SBD mixer / multiplier LO” arrangement would reduce frequency instability and phase noise on the transmitted signal, and would thus enable

synchronous demodulation of the data. For demonstration purposes, this could be done using offline processing. For OOK, synchronous demodulation theoretically will give only slightly improved sensitivity (~1 dB at BER = 10^{-3}). The real benefit for communications systems of developing low-phase-noise THz sources will be the ability to use phase modulated formats, such as BPSK or QPSK. This will require phase modulation of the output of one (or both) of the phase-locked lasers as illustrated in Figure 25. This would give an improvement in sensitivity (theoretically 3 dB for BPSK over OOK) or spectral efficiency (e.g. 10 Gb/s in ~5 Gb/s bandwidth with QPSK). Using offline and real-time techniques similar to those developed for coherent optical systems, synchronous demodulation of heterodyne (IF ≠ 0) or intradyne (IF ~ 0) signals could be performed.

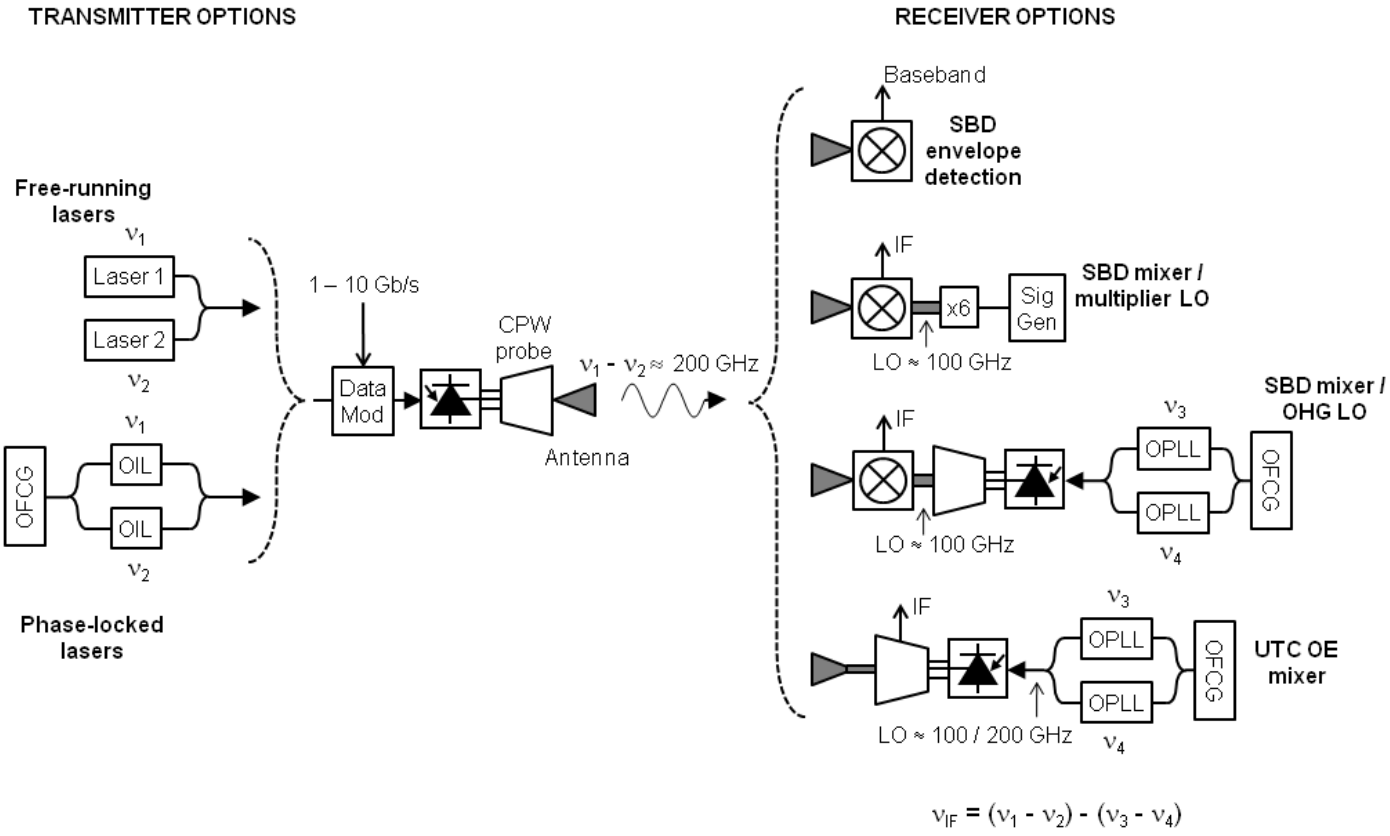

Figure 24: Possible experimental schemes for investigation of data transmission on ~200 GHz carrier.

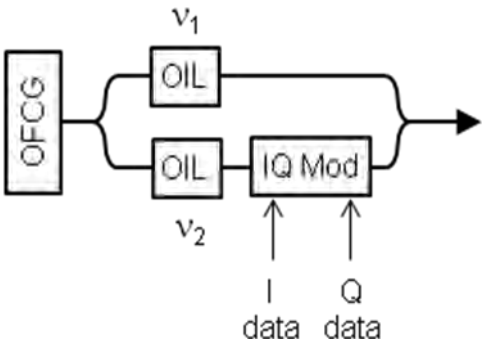

Figure 25: Photonic THz OHG source with in-phase and quadrature (IQ) modulation

7 SUMMARY AND CONCLUSIONS

This project has investigated the potential of photonic techniques for generating and coherently detecting millimetre and THz waves, with short-range (in-room) Gb/s communications systems that operate in unlicensed spectrum above 300 GHz as the target application. Ultimately, it is envisaged that this would allow compact, low-cost transceivers to be fabricated that leverage the mature InP-based photonic component and integration technologies that have been developed for optical fibre communications. Millimetre and THz signals can be generated with the precision and purity required for communication systems by optical heterodyne generation (OHG), in which the outputs of two phase-locked lasers are combined, and detection in a fast photodiode, such as a uni-travelling carrier (UTC) photodiode (PD). The same approach can be used to generate both a modulated carrier at the transmitter and an unmodulated local oscillator (LO) at the receiver. In this project, the UTC-PD has, for the first time, been extensively investigated as a down-converting optoelectronic mixer, with the aim of simplifying the receiver by combining the functions of LO generation and mixing in a single device that has potential for monolithic integration with OHG components.

Investigations into the UTC-PD as an optoelectronic mixer have been carried out mainly in the W-band (75 – 110 GHz), for which equipment is available commercially, simplifying signal generation and analysis. For down-conversion from 100 GHz, conversion gain as high as -32 dB has been observed at high photocurrent (~10 mA) and reverse-bias voltage (4 V). These operating conditions are necessary to achieve simultaneously significant non-linearity and wide frequency response. Furthermore, the conversion gain was observed to remain constant over more than five decades of input signal power variation. Although the conversion gain achieved is much lower than that obtained from more conventional mm-wave mixers (e.g. Schottky barrier diodes, which can achieve conversion gains > -10 dB), it represents a dramatic improvement over initial measurements performed early in the project that gave conversion gains below -60 dB. Future devices designed specifically to increase non-linear effects may allow the conversion gain to be further improved.

Qualitative and quantitative models of the non-linear processes giving optoelectronic mixing in the UTC-PD have been developed and compared against the experimental measurements. A computer model which predicts the conversion gain from DC current–voltage measurements made on UTC-PDs shows reasonable agreement with the experimental mixing results, but further development of this model is required to represent the frequency response of the UTC-PD accurately, which is a key factor in determining the conversion gain.

Sub-harmonic mixing experiments have demonstrated other modes of mixer operation, increasing the range of potential applications for the UTC-PD as an optoelectronic mixer. Harmonic mixing experiments have also demonstrated that the devices have a wide IF bandwidth (< 6 dB variation for IF from 5 – 23 GHz), a conclusion supported by fundamental mixing measurements at 80 GHz using a packaged UTC-PD with integrated bow-tie antenna, which showed < 3 dB variation of IF power across the IF frequency range 5 – 10 GHz.

Data transmission experiments have been carried out in which a UTC-PD has been used either as a down-converting mixer or a data transmitter. In the first case, BPSK was transmitted on an 80 GHz carrier at a rate of 500 kb/s, the data rate being limited by the low conversion gain achieved at that time (-74 dB) and the limited IF bandwidth imposed by the experimental arrangement. In a later experiment, an optical heterodyne generated by combining the outputs of two free-running external cavity lasers and OOK-modulated 1 Gb/s using an external electro-optic modulator was converted to a modulated signal at 200 GHz using a packaged UTC-PD. The signal was transmitted over a short (~2 cm) wireless link to a receiver consisting of an electrically pumped sub-harmonic Schottky barrier diode mixer, which down-converted the signal to an IF of 2.5 GHz. Offline processing was used to convert the signal to baseband and to perform bit-error measurements. A bit error rate (BER) of 10^{-3} was achieved for an estimated received power of -52 dBm. Based on the performance of this link, it

is estimated that transmission with the same BER should be possible over link lengths of more than 1 m at a carrier frequency of 300 GHz, provided the source power is greater than 0 dBm and total antenna gain of more than 40 dB is used. The required source power is challenging at 300 GHz using UTC-PDs, but potentially realisable in the short to medium term.

Overall, the results achieved in the project give us confidence that UTC-PDs, used as sources and/or optoelectronic mixers, will be a key component in future high-data-rate wireless communication systems at low-THz carrier frequencies.

LIST OF SYMBOLS, ABBREVIATIONS, AND ACRONYMS

AC	alternating current
BER	bit error rate
BPSK	binary phase shift keying
C	capacitance
C_{j0}	capacitance at zero bias voltage
CPW	coplanar waveguide
CW	continuous wave
DC	direct current
DFB	distributed feedback
DSB	double sideband
ECL	external cavity laser
EDFA	erbium-doped fibre amplifier
Gb/s	giga bits per second
IF	intermediate frequency
InP	indium phosphide
I_{ph}	photocurrent
IQ	in-phase and quadrature (modulation)
IV	current-voltage (diode characteristic)
LO	local oscillator
MZM	Mach-Zehnder modulator
OFCG	optical frequency comb generator
OHG	optical heterodyne generation
OIL	optical injection locking
OOK	on-off keying
OPLL	optical phase lock loop
PC	polarisation controller
PD	photodiode
P_{IF}	IF power
PRBS	pseudo-random bit sequence
P_{RF}	RF / mm-wave power (applied to UTC-PD)
Q	charge
QPSK	quaternary phase shift keying
RF	radio frequency
SEM	scanning electron microscope
SBD	Schottky barrier diode
SMA	sub-miniature version A (RF connector)
THz	terahertz
TW	travelling wave
UTC	uni-travelling carrier
V_b	bias voltage

REFERENCES

1. M. J. Fice, E. Rouvalis, L. Ponnampalam, C. C. Renaud, and A. J. Seeds, “Telecommunications technology-based terahertz sources,” Electronics Letters, vol. 46, 2010, pp. S28-S31.
2. E. Rouvalis, C.C. Renaud, D.G. Moodie, M.J. Robertson, and A.J. Seeds, “Traveling-wave Uni-Traveling Carrier Photodiodes for continuous wave THz generation,” Optics Express, vol. 18, May. 2010, pp. 11105-11110.
3. M. Fice, E. Rouvalis, R. Steed, C.P. Liu, C. Renaud, and A. Seeds, “Short range 10 Gb/s THz communications proof of concept”, Phase 2 Final Report, Award number FA8655-09-1-3078, September 2010.
4. E. Rouvalis, M.J. Fice, C.C. Renaud, and A.J. Seeds, “Optoelectronic detection of millimetre-wave signals with travelling-wave uni-travelling carrier photodiodes,” Optics Express, vol. 19, 2011, p. 2079–2084.
5. E. Rouvalis, M.J. Fice, C.C. Renaud and A.J. Seeds, “Optically pumped mixing at 100 GHz with travelling-wave uni-travelling carrier photodiodes,” Conference on Lasers and Electro-Optics (CLEO) 2011, Baltimore, 1-6 May 2011, paper JThB115.
6. A. Hirata T. Kosugi, H. Takahashi, R. Yamaguchi, F. Nakajima, T. Furuta, H. Ito, H. Sugahara, Y. Sato, T. Nagatsuma, “120-GHz-band millimeter-wave photonic wireless link for 10-Gb/s data transmission,” IEEE Transactions on Microwave Theory and Techniques, vol. 54, no. 5, 2006, pp. 1937–1944.
7. C. C. Renaud, D. Moodie, M. Robertson, and A. J. Seeds, “High output power at 110 GHz with a waveguide uni-travelling carrier photodiode,” LEOS 2007 - IEEE Lasers and Electro-Optics Society Annual Meeting Conference Proceedings, Oct. 2007, pp. 782-783.